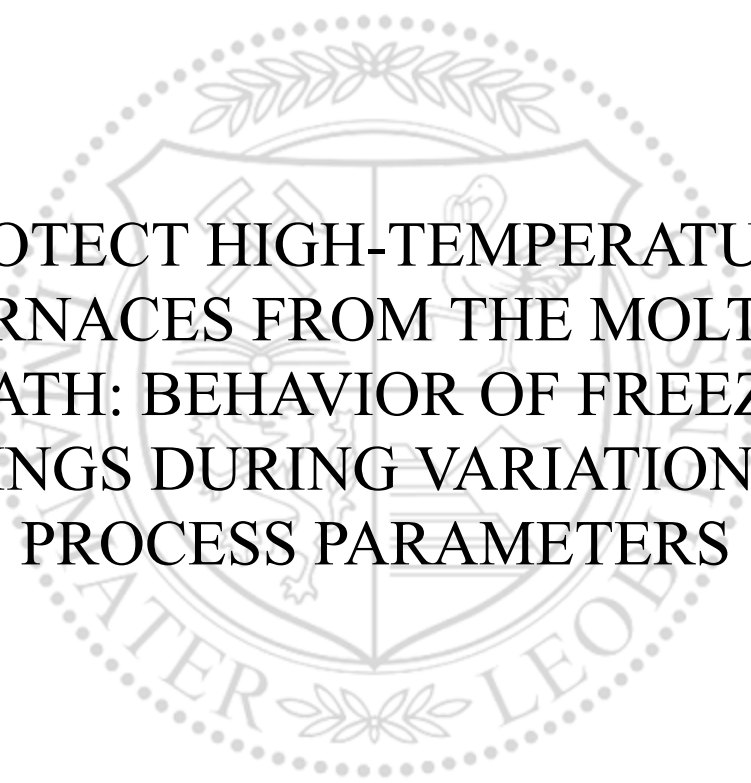Chair of Simulation and Modelling of Metallurgical Processes

Master's Thesis

PROTECT HIGH-TEMPERATURE FURNACES FROM THE MOLTEN BATH: BEHAVIOR OF FREEZE LININGS DURING VARIATIONS IN PROCESS PARAMETERS

Abdul Razziq

September 2023

PROTECT HIGH-TEMPERATURE FURNACES FROM THE MOLTEN BATH: BEHAVIOR OF FREEZE LININGS DURING VARIATIONS IN PROCESS PARAMETERS

Abdul Razziq

Thesis submitted for the degree of
EIT-KIC Master of Science in
Sustainable Materials, option
Sustainable Metallurgy
(Leoben-Leuven)

Supervisors:
Prof.dr.ir. Bart Blanpain
Dr.ir. Annelies Malfliet

Assessors:
Dr.-ing. Menghuai Wu
Prof.dr.ir. Nele Moelans

Assistant-supervisors:
ir. Gaëlle Butin
Dr.ir. Lennart Scheunis

Academic year 2022 – 2023

AFFIDAVIT

I declare on oath that I wrote this thesis independently, did not use other than the specified sources and aids, and did not otherwise use any unauthorized aids.

I declare that I have read, understood, and complied with the guidelines of the senate of the Montanuniversität Leoben for "Good Scientific Practice".

Furthermore, I declare that the electronic and printed version of the submitted thesis are identical, both, formally and with regard to content.

Date 19.09.2023

Signature Author
Abdul Razziq

Contents

List of Figures

List of Tables

Abstract

It has been demonstrated that the use of freeze lining technologies can significantly increase the working lives of pyrometallurgical furnaces that are subjected to demanding process conditions and corrosive liquid melts. By cooling the outer furnace walls, the freeze linings on the inner walls of the furnace linings can be formed. Both the thickness of the freeze lining and the heat loss through the furnace walls, are of special concern to process operators.

The aim of this thesis is to investigate the effect of transition of spinel primary phase field slag to melilite primary phase field slag and vice versa on freeze lining formations in terms of microstructure and thickness of freeze linings. Until now a lot of research has been done for the formation of steady state freeze linings and temperature at the interface. But there needs to be done intense amount of research in transient state freeze linings because this could be useful for numerous recycling smelting refineries where the secondary raw material is coming from different sources which is used as a batch feed for recycling of precious metals. Hence, there is a high chance of change in slag bath and how it effects the already formed freeze linings needs to be studied.

The slag system chosen in this thesis is the SiO_2-FeO-CaO-Al_2O_3 system. The slag compositions are selected to be in either the melilite or spinel primary phase field. FactSage simulations are done to find out suitable compositions of slag. First, the time needed to form a steady state thickness in a specific primary phase field freeze lining is determined which was found out to be probably 3 hours. After that, the transition of slag composition is done by the initial formation of a freeze lining in one specific primary phase field and then inserting it into the molten slag bath of another primary phase field composition. Microscopic characterizations are performed to investigate the freeze linings. In case of the transition from the spinel primary phase field slag to the melilite primary phase field slag, microstructure of the crystalline layer remained similar compared to the spinel primary phase field intermediate freeze lining before the transition. But there is a formation of an open crystalline layer between the crystalline layer and the slag bath. The open crystalline layer is composed of already formed undissolved anorthite and spinel crystals similar to the open crystalline layer and an entrained slag bath layer before the transition but with the solidified slag matrix where Spinel primary phase slag and melilite primary phase slags got mixed up. Also, there is a precipitation of new melilite phase after the transition in the nearby region of slag bath. In case of the transition from the melilite primary phase field slag to the spinel primary phase field slag, the microstructure of the crystalline layer is again similar to the initially formed intermediate freeze lining in a melilite primary phase field slag before the transition. But after that a closed crystalline layer is formed instead of an open

crystalline layer and an entrained slag bath layer which was formed before the transition. In this closed crystalline layer, there are large sized grown crystals of Ca-pyroxene, spinel and anorthite crystals which extend up to around 1 mm of thickness from the endpoint of the crystalline layer. But in the melilite primary phase intermediate freeze lining before transition, these phases were present with a smaller size over a shorter region. Also, after the transition, there is a growth of second generation of anorthite crystals in the closed crystalline layer which was not there in the intermediate melilite primary phase freeze lining before the transition. Furthermore, in the region nearby the slag bath in the intermediate freeze lining after the transition, there is a formation of large volume of melilite crystals with already present undissolved anorthite and the spinel crystals with the solidified slag matrix where Spinel primary phase slag and melilite primary phase slags got mixed up. Whereas before the transition, only anorthite and spinel crystals were present in the region nearby the slag bath. In both experiments of transition from the spinel primary phase field slag to the melilite primary phase field slag and vice versa, there is no formation of a freeze lining of different slag composition on top of the initially formed intermediate freeze lining in a specific composition. The outcome of these experiments will be useful to understand the change in behavior of freeze linings while changing the slag bath in a quaternary system.

Chapter 1

1. Introduction

Non-ferrous metals recycling in general is extremely vital for the environmental sustainability. Only 3% of the required primary raw materials are produced by the EU. The EU's metal recycling value chain reduces the dependency of the EU on imported materials. Recycling reduces landfilling and it's the related costs, avoids the loss of valuable raw materials, and has a huge positive impact on the environment. It results in a significant reduction in CO_2 emissions. [1]

The following challenges can be encountered by the EU in terms of non-ferrous recycling: Difficulty to implement innovative technologies and avoid investment leakages. According to the 2050 vision, the non-ferrous metals industry would like to be a key player in closing the resource loops. But there will be hurdles in the reprocessing, collection, and disassembly of scraps. [2]

Figure 1.1 shows the non-ferrous metals recycling flowsheet of Umicore Hoboken. This company uses a pyrometallurgical furnace which is named ISASMELT. The molten slag in this furnace can cause excessive wear of the refractory lining. If the parameters for the formation of stable freeze linings could be set, the cost of excessive changing of the refractory lining can be saved.
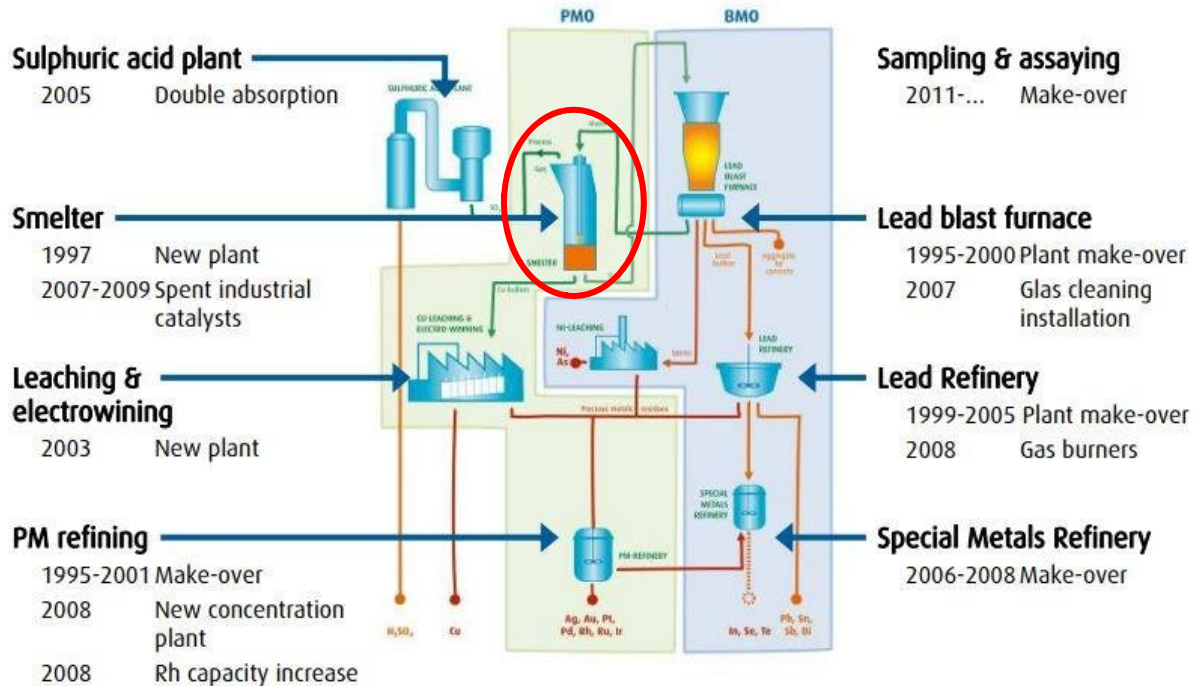
Figure 1.1 *Flowsheet of the Umicore Hoboken plant [3]*

Since 1995, "freeze linings" received recognition, because of their durability and economical importance. [4] The formation of a protective layer on the refractory's hot face by freezing the process material due to an efficient cooling design is known as freeze lining. To get a freeze lining, the temperature of the hot face must be less than the liquidus temperature of the materials present in the slag. The obtained freeze lining will become the actual lining instead of the refractory lining already present, if somehow the frozen deposit is stable. In this way, it will protect the main refractory lining from wear, hence improving its life. Moreover, freeze linings can also be formed directly on cooling plates in the case of the furnaces where there is no refractory lining. [5]

The removal of heat via the cooling system and the input of heat from the molten bath is in balance for the steady state freeze linings as shown in **Figure 1.2**. If the heat input is higher than the heat removal, the freeze-lining will wear out, while if it is lower, the freeze lining will grow. [6]
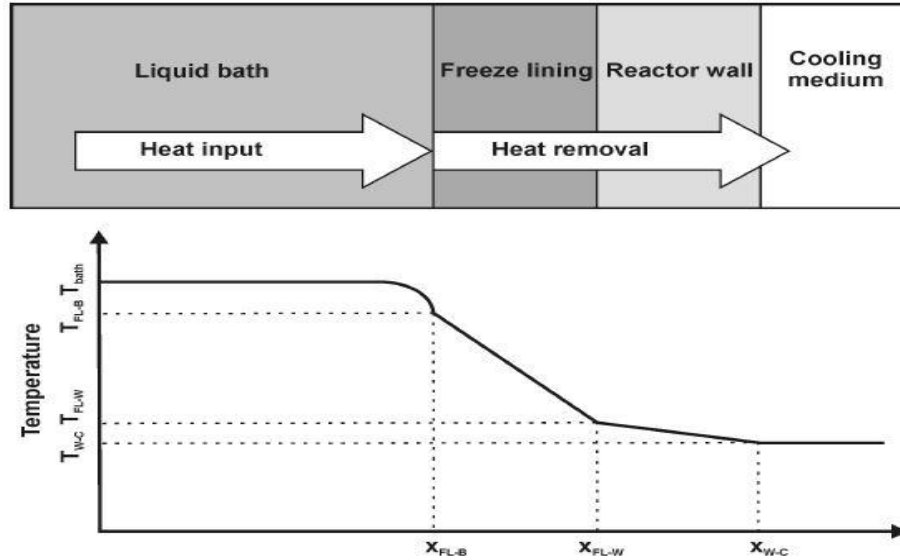
Figure 1.2 *Temperature profile of the freeze lining which is in continuous contact with a liquid bath. $T_{W\text{-}C}$: Temperature at reactor wall-cooling medium interface, $T_{FL\text{-}W}$: Temperature at freeze lining-reactor wall interface, $T_{FL\text{-}B}$: Temperature at bath-freeze lining interface, T_{bath}: Bath Temperature, $X_{FL\text{-}B}$: Bath-freeze lining interface position, $X_{FL\text{-}W}$: Freeze lining-reactor wall interface position , $X_{W\text{-}C}$: Reactor wall-cooling medium interface position. [6]*

Objectives

A lot of research in the past has been focused on the formation of freeze linings in steady state in terms of the slag composition and the application of freeze linings in different furnaces, as well as on the heat and mass transfer in freeze linings. This research is done to predict the change in behavior of freeze linings during varying process parameters by doing lab scale experiments for the Al-Ca-Si-Fe-O slag system. Change in slag bath composition in terms of primary phase field will be done in this research. The main objective is to analyze the evolution of the microstructure in a freeze lining when there is a change in slag bath. For achieving this goal, transition experiments are performed by forming a freeze lining in a specific primary phase field followed by its submergence in another primary phase field slag.

Chapter 2

2. Literature Study

In this chapter, the current knowledge of the freeze linings for different industrial furnaces is discussed which includes detailed freeze lining and the efficient cooling designs to achieve stable freeze linings. Moreover, research done at lab scale regarding the heat transfer phenomenon, solidification mechanisms, different stages of growth and the effect of varying parameters on freeze lining formations is discussed. Section 2.1, 2.2, 2.3 and 2.4 focuses on the industrial use of the freeze linings. Whereas the other sections after that are focused on the lab scale investigations on the formation of freeze linings in terms of the microstructures and under varying process parameters.

2.1. Overview on current freeze linings investigations among different type of furnaces

2.1. a) Blast furnace

The effect of various process materials on the freeze lining behavior in a blast furnace has been studied, such as the effect of incoming dust and volatile components on the formation of a freeze lining or of dust on the erosion of the freeze lining. [7] [8]

Under changing process conditions, i.e., bath temperature or process material composition, studies on the stability of freeze lining are of vital interest to protect the refractory materials. Until now, for the blast furnace process, the research is focused on corrosion prevention but not so much research is considering the effect of the changing process parameters such as the composition of the process materials. [9] [10]

2.1. b) Steel convertor

In this process, the bath temperatures are extremely high because of the exothermal oxidation reactions caused by the addition of oxygen to remove the surplus carbon and certain impurities. Consequently, the conditions are aggressive for the refractory material which makes freeze lining a viable solution.

In the convertor, freeze linings are formed by splashing of the remaining slag after removal of the steel melt on the refractory walls (**Figure 2.1**). As this is a batch process, there is a continuous change in the process conditions in the reactor vessel which makes the freeze lining stability highly vulnerable. Knowledge on the transient freeze lining behavior is therefore important. [11]
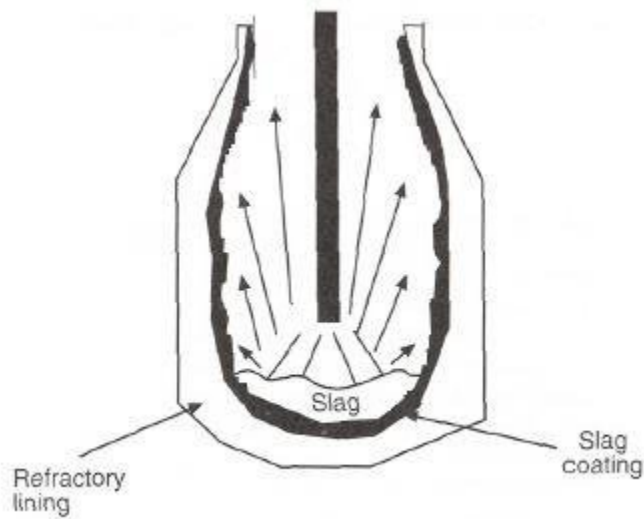
Figure 2.1: Formation of slag coating (freeze lining) on lance and the reactor wall due to splashing of slag. [12]

2.1. c) Hall- Héroult process

Various thermal [13] and physical [14] models have been formulized for the Hall–Héroult process. For the bath-freeze lining interface temperature, the electrolyte liquidus temperature is considered and it is assumed that the mass transfer and crystallization will occur hastily.

Research on freeze linings microstructure has shown that the growth rate has a high influence on the freeze lining composition and during some growth rates, dendrite growth can be seen. [15]. Furthermore, instead of steady state studies to investigate freeze linings, a transient state study can be more crucial for the formation of freeze linings as depicted by the transient models which include mass transport. [16]

2.1.d) Zinc fuming process

The zinc fuming process requires a thoroughly mixed high temperature slag bath to enable and maintain the high fuming rate. As, Zinc must be removed in its gaseous form because of its high volatile property. Therefore, the use of freeze lining is necessary to protect the refractory materials at such high temperatures.

In the studies done by Verscheure [17], the bath-freeze lining interface temperature was predicted. He found out that the second phase must be formed according to the phase diagram other than the primary phase was also present at the bath-freeze lining interface, which shows that for some processes it is possible that the bath-freeze lining interface temperatu is lower than the bath liquidous. This should be kept in mind when designing simulation models. It has also been found out that slag engineering can improve the freeze lining performance.

5

2.1.1. ISASMELT furnace

The Isasmelt furnace is a steel vessel lined with refractory bricks in an upright-cylindrical shape as shown in **Figure 2.2**. A molten bath of slag is present at the bottom of this furnace as well as copper matte in molten form in case of copper recycling [18]. A steel lance is inserted and lowered into the bath from a hole at the top surface of furnace. Strong agitation of the bath occurs because of the oxygen-enriched air injected through the lance. Materials which are to be recycled are dropped through another hole in the roof of the furnace or in some cases injected through the lance itself. As a result, there is an intensive reaction between the oxygen and the materials for recycling. [19]

Early development

Back in 1973, the invention of the Sirosmelt lance by Dr John Floyd and Dr Bill Denholm at CSIRO lead to the foundation of the ISASMELT Furnace processes. At that time, it was developed during a study to enhance the tin-smelting process. [20]

Back in 1902, this idea of top-entry submerged lances was implemented in France, but it resulted in a failure because of the detrimental effect of the slag bath on the surface of the lances resulted in short lives of the lances. The Mitsubishi Copper smelter also used a top lance inserted from the furnace roof but without inserting it in the molten bath, this however didn't fulfil the cause because of insufficient mixing of the bath. by blowing oxygen-enriched air but this doesn't fulfil the cause because of insufficient mixing of bath. [19] [21] The submerged lance smelting was made successful only after inclusion of swirlers in the lance or the coating of slag on the outer surface of lance caused by splashing.

Figure 2.2 *Cross sectional view of the isasmelt furnace via xstrata technology. [19]*

Commercial primary copper ISASMELT smelters

The first commercial primary copper ISASMELT furnace plant was made by a company named Agip at Mount Isa in western Australia in 1990. This plant was designed to produce 1.5 tons/h of matte in granulated form with combined copper and nickel content of 45% for sale. But it had to be closed because of low nickel prices. [22]

The third commercial ISASMELT plant for copper was started at Mount Isa Copper smelter in August 1992. The capacity of this plant was to treat 104 tons/h of copper concentrate leading to 180,000 tons/y of copper. The major difference among Mount Isa ISASMELT copper plant and others was that it is equipped with an Ahlstrom Fluxflow waste heat boiler in order to recover the heat energy from the outgoing waste gases. [23]

Commercial ISASMELT smelter plant for secondary copper

Umicore

Umicore built their Hoboken smelter site which is close to Antwerp, Belgium. This new plant was started in 1997 and was having a capacity to treat 300,000 tons/y of secondary materials. This plant significantly reduced the operating cost of the whole plant by substituting a roasting plant, one sulfuric acid plant, a copper blast furnace, a sinter plant and four Hoboken convertors.

In the first step of the Umicore Hoboken plant, feed materials are oxidized to form a Pb-rich slag and copper matte, then the slag is tapped and reduced in a blast furnace to produce lead metal followed by conversion of copper matte into blister copper. Whereas, The copper is passed to the refining process resulting in pure copper metal. [24]

2.2. Potential of freeze lining in ISASMELT process

By injection of gas using a submerged lance in the ISASMELT furnace, high convective conditions are achieved which in turn are extremely hazardous for the lance material. Therefore, its ability to form a protective layer of solidified molten bath on its outer surface is an important design criterium. Some research has been done in past to calculate the heat convection coefficient by considering the heat transfer through the solidified slag layer. Bath-freeze layer interface temperature assumed to be at the liquidous of the molten bath to calculate the heat convection coefficient. It was also found out that this solidified freeze lining is mainly composed of magnetite, with a small amount of fayalite (Fe_2SiO_4) and also glass. [25]

In all these studies, the assumptions of the models are based only on heat transfer and steady state conditions without any impact of the variations in slag compositions. For the ISASMELT furnace in the Umicore Hoboken plant, it is necessary to include mass transfer in the research models with transient state conditions and slag engineering because in the application there is varying feed of secondary raw materials sources.

2.3. Cooling designs and the materials for non-ferrous metals furnaces

There are various cooling designs to cool down outer shells/walls of the non-ferrous metals furnaces, such as:

2.3.a) Spray/shower coolers

This type of cooling for furnaces has both advantages and disadvantages. In simple words, it is just a water spray on the outer shell of a furnace. Because it is inexpensive, it has been used extensively in the non-ferrous metals industry. [26] The main advantage is that the system can be installed at any time without the need of creating any extra hole from the outer steel shell of furnace.

However, as the cooling is done from the outside, there is extremely restricted effect onto the hot face of refractory lining which results in its wear. The reason for that is temperature of hot face is not decreased to a less value in comparison to liquidous of molten slag bath. Consequently, the thickness of the refractory lining reduces to a few centimeters which is not enough. Another critical issue is the furnace wall deformation, due to thermal stresses from the heat removal through the furnace shell. [26]

2.3.b) Internal block/rings

Internal blocks or rings are made from copper and placed within the refractory. They come in various designs, for instance, in the form of rings, small remote blocks dispersed throughout the furnace or straight long sections. Most common use of them is in non-ferrous furnaces. [27]

The main problem that is encountered using these internal blocks as coolers is the risk of water leakage leading to steam explosion. Also, there can be uneven wear of refractory lining because of localized cooling and the low thermal conductivity of refractories hinders the uniform cooling.

2.3.c) Panels

They are applied under the slag line done in non-ferrous applications. Currently, they are used mostly in Zinc slag fuming process. However, to an extremely limited extent. [26]

In a modified design, a layer of refractory is combined with large copper blocks. The key difference among various designs is the use of a particular profile on the hot face to maintain the slag layer or the refractory as shown in **Figure 2.3**.The foremost challenge is to maintain a protective layer on metal due to its low conductivity and thermal cycling [28]
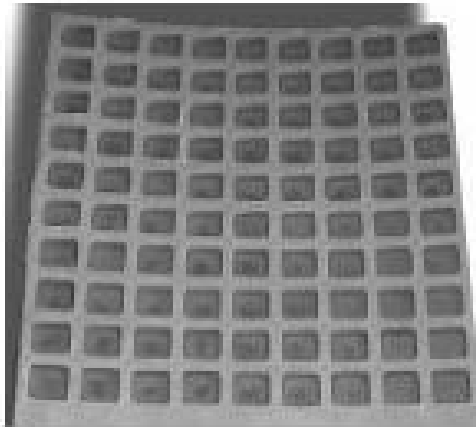
Figure 2.3 Hot face pockets for the entrapment of refractory or slag. As cast electric arc furnace wall cooling panel.
[29]

2.3.d) External jackets

External jackets act as a temporary measure for the cases where a threatening level of wear has been reached. They are mostly used as an alternative to the spray/shower cooling type. They have the same

drawbacks as discussed for spray/shower coolers with in addition that hot spots cannot be detected with the naked eye.

The applicability of specific metals as furnace coolers depends highly on the amount of cooling that is needed in a particular process. Cast iron and steel are often used when not much cooling is required. Depending on the required thermal and mechanical properties, nodular cast iron or grey iron are being used. In the furnace shells which are used in shower/spray coolers, high strength is required with not much of cooling, and as a result steel is used to make them.

Copper is also extensively used as a coolant material because of its higher thermal conductivity. But its purity is a main concern because even a very small amount of impurity can have detrimental effect on its thermal conductivity. Often steel and copper are combined but extra precautions are needed for that purpose because of the chance for galvanic corrosion to occur. [30] Some research has also been done to combine 4% aluminum with copper in order to decrease the effect of corrosion but there was a 40% decrease in the thermal conductivity which restricted it to be used as an alloy. [30]

2.4. Cooled probe technique for experimentation

For all other methods to study slag solidification such as:

- Single hot thermocouple technique
- Confocal scanning microscopy coupled with a high temperature reaction cell
- Double hot thermocouple technique

There are various limitations which include, some nonferrous slags contain iron oxide, which renders the slags opaque, rendering some procedures useless. The temperature control occurs throughout the system, preventing the imposition of a temperature gradient. Additionally, they frequently investigate small sample sizes, which could affect the cooling path (note that in reality, the lining is in contact with a large molten bath with an almost constant composition) [31]

The cooled-probe approach, which may be used to produce freeze linings under controlled atmospheric conditions in a laboratory setting and to analyze the generated microstructure and its growth, is exempt from these restrictions. The bath is first melted in a furnace, then the cooled probe is dipped into the molten liquid, where the lining begins to harden on it because of cooling. Complete quenching of the produced lining is followed by microstructural and phase studies of the deposit. [32]

Thonstad and Rolseth [31] made the first reference to their study of the microstructural evolution using this kind of setup. To look at how side ledges arise in cryolite, they used a cooled wall rather than a cooled

probe. This was carried out in a steel laboratory cell that could withstand heat. By running an AC current between two steel rods that were dipped in the cryolite melt, the melt was heated. The cold wall was first insulated along with the molten full bath, and the insulation was then removed, leaving a ledge on the cold wall. Using X-ray diffraction, X-ray fluorescence, and wet chemical analysis, respectively, the phases present in the ledge and the bulk ledge composition were identified.

A probe that was air-cooled and made of stainless steel was utilized by Solheim and Sten [31]. This probe was used for more practical reasons since it was much easier to insert the probe once the melt had been sufficiently heated (5–15 °C above the liquidus of the bulk melt) than it would have been to work with a cooled wall. The furnace controller was set 15 °C higher to account for the probe's cooling of the melt. The deposit's real microstructure wasn't examined either, but samples of the deposit were taken for study by flinging the deposit at various distances from the probe's surface.

Verscheure [33] refined the experimental setup even more by spinning the crucible that held the liquid bath into which a cooled probe was inserted to create a solidified layer. This makes the apparatus more closely connected to the industrial system and subjects the slag to a similar temperature gradient and cooling trajectory while also allowing for the investigation of the fluid flow and its effects. Through forced convection, the crucible rotation improves the bath's temperature and compositional uniformity.

Given that crucible type is a crucial variable in all pyrometallurgical investigations, this choice turned out to be extremely significant. For instance, Jansson [34] discovered significant difficulties with the trials with industrial calcium ferrite slag. This occurred because the slag's viscosity was too low to prevent slag leaking. They did so by showing how, as the crucible heats up, some microcracks appear and then grow larger because of the fast dissolving of magnesia into the molten slag.

Focus was on the freeze-lining formation kinetics and processes with direct growth on a cooled metal surface of the probe in most experiments using the cooled-probe approach. This is only true for a portion of industrial freeze linings, though, as many designs include a brick layer between the molten bath and the cooler or refractory bricks in the construction of the cooling equipment. For this reason, Kalliala [35] wrapped a ceramic refractory liner sleeve around the probe. Due to the different thermal expansion coefficients of the metal probe and refractory sleeve, as well as the assembly-required tolerances, an air gap was produced, which dominated heat transfer. Due to the altered heat transmission circuit and higher average temperature of the refractory, the slag was no longer able to remain molten in the refractory's open porosity, which allowed it to swiftly penetrate the pore system. The studies only involved a 30-minute immersion period, yet even this was sufficient for the molten slag to enter the refractory sleeve's open

porosity. It is obvious that the refractory sleeve's presence decreased the thickness of the freeze-lining. The lining's microstructure was also considerably more homogeneous throughout the layer.

2.5. Heat transfer phenomenon through freeze linings

In the past research [26] [36] that has been done in the field of freeze linings, it has been assumed that formation of freeze lining is supported by thermal balance among heat output through the cooled furnace wall Q_{wall}, heat input from the superheated Slag bath Q_{bath} and the latent heat of fusion at the hot face of freeze lining Q_{fusion}. If we express all this in an equation, then we get the following equation:

$$Q_{bath} + Q_{fusion} = Q_{wall} \qquad (1)$$

If we only consider 1D (one-dimension), these heat fluxes can be expressed as follow:

$$Q_{bath} = h_{bath} * A_{bath} (T_{bath} - T_{liquidus}) \qquad (2)$$

$$Q_{fusion} = \rho * H_f * \frac{dt_{fl}}{dt} \qquad (3)$$

$$Q_{wall} = k_{fl} * A_{bath} * \frac{dT}{dx}|_{hotface} \qquad (4)$$

Where,

h_{bath} =Coefficient of convection from bath to freeze linings

A_{bath} = Interface area bath/refractory

T_{bath} = Bath temperature

$T_{liquidus}$ = Liquidus temperature of bath material

K_{fl} = Freeze lining thermal conductivity

T = Local temperature in the freeze lining and the wall

ρ = Freeze lining density

H_f = Latent heat of fusion

t_{fl} = Freeze lining thickness

$\frac{dT}{dx}|_{hotface}$ = Freeze lining thermal gradient evaluated at the freeze linings hot face

From the above-mentioned equations from 1-4, it can be seen easily that if there is some disturbance in Q_{wall} or Q_{bath}, it will be compensated either by Q_{fusion} (bath materials solidification to freeze lining or the melting of freeze linings). For example, if there is an abrupt decrease of Q_{bath} via rapid decrease of bath temperature, this will result in solidification of extra bath material to the freeze lining ($Q_{fusion} > 0$). Likewise, a sudden increase in Q_{bath} due to sudden increase in the bath temperature will result in the melting of freeze lining ($Q_{fusion} < 0$). [26]

2.6.   Slag solidification mechanism

The process material must create a solid coating on the reactor wall for a freeze lining to be stable, but more critically, this layer must continue to be adhered to the refractory wall. If this layer does spall, a new layer should form right away. Ideally, this layer shouldn't. This behavior of the freeze lining is dependent on the development of the freeze layer and its thermal history, which are shown in the microstructure. The physical, mechanical, and chemical characteristics of the freeze layer are also influenced by its local microstructure, which also affects its performance and stability. [6]

The easiest way to explain why the freeze lining's local microstructure is crucial is with an example: the microstructure will influence the freeze lining's melting. For instance, big crystals of a phase with a different composition from the slag bath will melt more slowly than a glass phase with the same composition as the bath. [6]

A cooled-probe approach is often used to study freeze-lining formation. The complicated microstructure of the solidified layers changes with distance from the probe. The solidification mechanism and, consequently, the final microstructure are influenced by the solidification velocity and temperature gradient at the liquid/solid interface. While the freeze lining is forming, the temperature gradient and solidification rate are continuously shifting, creating various zones:

- "Zone 1" refers to the area with an amorphous matrix and small precipitates that is closest to the cooled probe.
- "Zone 2" to the area with equiaxial crystals.
- "Zone 3" to the area with columnar crystals.

- "Zone 4" to the area with an amorphous matrix and small precipitates that is close to the liquid bath. [6]

The local temperature and its relationship to the distance to the probe should be considered to comprehend the growth of freeze-linings. Due to its proximity to the cooled probe, the slag on the cooled-probe side cools down quickly to a low temperature, whereupon a glass phase is created. On the probe, this solidified slag layer then serves as an insulating layer. As a result, the temperature rises as you get further from the probe. As a result, the next slag layer solidifies later and at a higher temperature. [6] The temperature changes in a manner that is graphically depicted in Fig. 2.4

The solidified slag is annealed at the higher temperatures farther from the probe, as is depicted in Fig. 2.4 for longer submergence times. This means that the microstructure of the frozen layer may continue to coarsen over time, depending on the location. Later, this was confirmed by Jansson [37]. The glassy structure was crystalline in nature. The frozen layer rapidly cools to ambient temperature when the probe is removed from the bath, as seen by the gray lines in **Figure 2.4**, beginning at time t1. It is believed that the microstructure will only be slightly impacted by this cooling. Crystal growth is made feasible by greater temperatures farther from the probe, but this also depends on mass transport. [6]
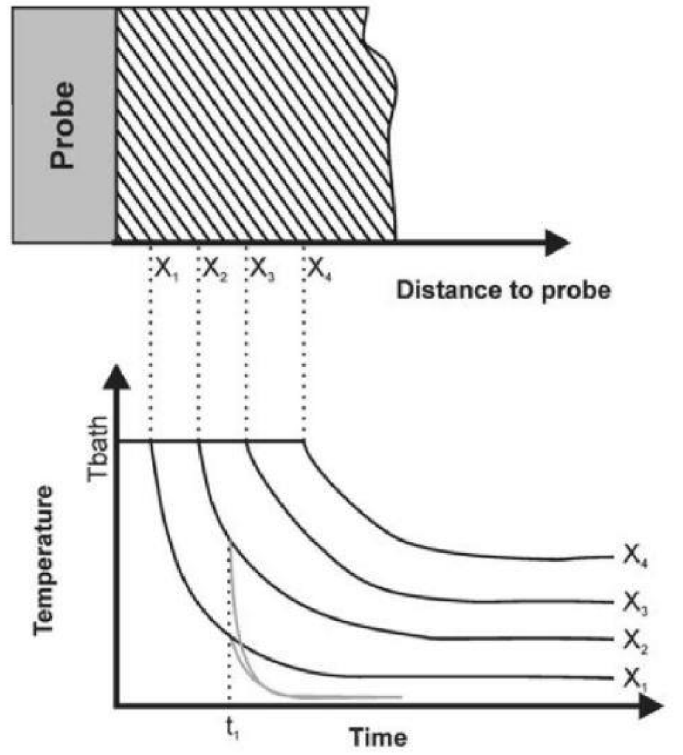
Figure 2.4 *For varying distances (x1 through x4) from the probe surface, the temperature evolution in a frozen layer as a function of time is depicted schematically in the drawing. The evolutions during the experiment are shown by the black curves, and the evolutions following the removal of the probe from the liquid bath at time t1 and the subsequent cooling to room temperature are shown by the gray curves. [6]*

One can distinguish between short-range mass transport, where the local mass exchange between glass and crystals doesn't affect the freeze lining's global composition, and long-range mass transport, where the mass exchange occurs parallel to the heat flux and affects the composition of the freeze lining globally. It is expected that only short-range mass movement takes place in the layers closest to the probe and, therefore, at lower temperatures (glass phase and glass with equiaxed crystals in it). The growth of the columnar crystal layer is influenced by long-range mass transport. However, keep in mind that in addition to the mass movement of the major components, the mass transport of minor components can also have a significant impact. [37]

According to Campforts [6, 38], the general solidification theory and the continuously shifting solidification conditions explained how the crystal form and scale changed within the layers. The temperature gradient at the solid-liquid interface (G)and the solidification rate (V) are two crucial variables. The ratio of those two (G/V) determines the growth morphology. A planar front develops at high G/V, then as G/V falls, branchless columnar crystals, dendrites, and finally equiaxial crystals are formed at low G/V. The product

GV determines the microstructure's scale. Fine grains are produced for high values, while coarse grains are produced for low values.

The liquid slag in zone 1, which is closest to the cooling probe, is swiftly quenched and is virtually in direct contact with the hot bath. The temperature is still relatively high in that area at the time of submersion, resulting in a low G/V ratio and a high GV value. This causes a tiny number of microscopic crystals to form after quenching, resulting in an amorphous phase that makes up most of the microstructure. In this region, the composition of the bath and the freeze layer are identical. The size of the crystals can vary, but it Is independent of immersion time. Thus, it is not because the crystals have been annealed; rather, it may be because there is less contact between the probe and the lining, which causes the slag to sometimes cool more slowly and allow for the formation of slightly coarser crystals. If temperatures below liquidus are employed, some of the bigger particles may also be present. [6]

Zone 2 produces a higher G/V and a lower GV than zone 1 since the temperatures there are lower at the time of development. As a result, larger equiaxial crystals than in zone 1 develop. There is also an amorphous matrix present in the spaces between the crystals. In this zone, no annealing effect is seen either. This area of the freeze liner has the same chemical composition as the bath. [6]

Zone 3 has a higher G/V ratio, allowing columnar crystals to form. But this indicates that the growth of the layer is governed by mass movement as well as heat transport. Concentration gradients may develop in the liquid at the solid-liquid interface if the solidification rate is comparable to or less than the mass transport rate. Due to a localized increase in liquidus temperature at the solid-liquid interface, columnar growth may develop in a region of constitutional undercooling. Additionally, GV falls even more, leading in bigger columnar crystals. The composition of the frozen layer in zone 3 differs slightly from the composition of the bath during longer submergence times. [6]

A second amorphous matrix with tiny crystals is seen in zone 4. when the probe is removed, liquid slag from this zone adheres to the frozen layer. [6]

Different growth mechanisms that correspond to different crystal structures also have implications. For example, while some crystals, like olivine, form an open network of long thin crystals with a large amount of matrix in between the crystals, others, like melilite, form a closed network of large broad crystals with a small amount of matrix in between. To expand in a closed network, the liquid slag bath and the freezing layer must exchange materials. In an open network, the solid layer and the regional matrix between the crystals can exchange components. [37]

It is found out, in a study on slag solidification in continuous casting process [39] that the slag layer consists of three layers: liquid, a glass and a crystalline layer with their thickness depending upon composition of the slag. Moreover, the bath/freeze lining temperature was found out to be lower than the liquidus temperature. Also the cooling rate plays a vital role which makes slag solidification behavior highly dependent on the local thermal conditions. Consequently, we can say that the crystallization behavior is of high importance to be investigated along with the bath/freeze lining interface. [39]

Also, the behavior of steady state freeze lining is determined by elementary reaction steps and rates of mass transfer, crystallization pathway, crystallization rate, nucleation and phase transformations and equilibria in a reaction system. [5] While doing the freeze lining research considering a concentrated $CaCl_2$ aqueous solution, there was no effect of changing the bulk fluid flow but a change in bath temperature, thermal history of the deposit and the bath composition highly affected the phases formed, the freeze lining thickness and the interface temperature. [5]

M. Campforts et al. [40] differentiated the formation of various layers generally observed in a freeze lining. For the slag compositions shown in **Table 2.1**, the seven distinguishable layers are shown in **Table 2.2**.

Table 2-1: *Six different slags with varying amounts of CaO, SiO2, PbO, ZnO, Fe2O3 and Al2O3 in their compositions [40]*

Slag	CaO	SiO_2	PbO	ZnO	Fe_2O_3	Al_2O_3
M1	12.0	11.0	48.0	4.0	22.0	3.0
M2	11.7	16.3	50.5	8.3	13.2	0.0
M3	17.0	26.0	39.0	5.5	10.5	2.0
S1	4.0	11.0	58.5	3.5	20.5	2.5
S2	13.3	22.4	44.8	5.7	11.3	2.5
S3	8.0	25.3	50.5	4.1	9.5	2.5

Table 2-2. Names of the seven layers with their microstructural characteristics formed in a freeze lining for specific slag compositions [40]

Number	Name	Microstructural characteristics	Slags
(1)	Glass layer	Only glass phase is observed	Mx and Sx
(2)	Glass with crystals layer	Equiaxed crystals are present in the glass phase	M1, M2 and Sx
(3)	Crystalline layer	The slag is fully crystalline	M1, M2 and S1
(4)	(First) "crystals in liquid layer"	Crystals that are interlocked and that contain liquid in between	Mx, S1 and S2
(5)	Sealing crystals layer	Large broad crystals that form a dense layer	M1, M2 and S2
(6)	Entrained slag bath layer	Similar to the glass layer, but located at the bath side of the freeze lining	Mx and Sx
(7)	Second "crystals in liquid layer"	Crystals that are connected and that contain liquid in between	M1

Figure 2.5 shows the formation of 6 different layers formed after 120 min of N2 cooled probe insertion in a molten slag bath. [38] These layers are numbered in same order as mentioned in Table 1.2. The distance to the probe is explained through the scale bar at the bottom of the image. Furthermore, **Figure 2.6** is the zoomed in part of layer 4 which confirms the formation of four crystalline phases Spinel, Melilite, PCSi (Polycarbonate silicate), PbFe (Arrojadite) and glass phase in it. [40]
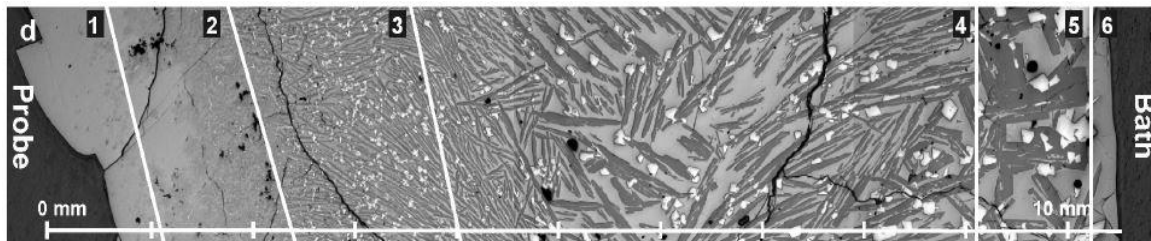
Figure 2.5 Light optical microscopy image of freeze lining after 120 minutes. (1) Glass layer (2) Glass with crystals layer (3) Crystalline layer (4) First "Crystals in liquid layer" (5) Sealing crystals layer (6) Entrained slag bath layer [38]
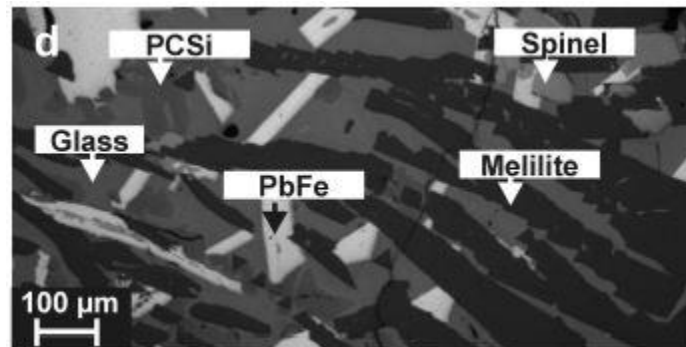
Figure 2.6 Detailed Microstructure of Layer 4 as shown in Figure 2.4 [40]

2.7. Different stages in freeze lining growth

To start off with, a high viscosity liquid layer is formed as shown in **Figure 2.7** and this growth is dominant before the slag crystallization occurs. For some slags with higher viscosities usually with higher SiO2 concentration, the glass layer is dominant for the long times during freeze lining growth which means a delay in formation of crystals. Followed by the formation of non-interlocking crystals in high viscosity layer. In the next stage interlocking crystals are formed in the glass layer. In the fourth stage, both the interlocking melting crystals which have low melting point and non-interlocking non-melting crystals which have high melting point are found in the liquid layer. A sealing crystal layer consisting of high melting interlocking phase is formed in the fifth stage. Finally, after the formation of crystals in the liquid layer, a high melting phase layer is formed whose interlocking crystals differ from the crystals in the liquid layer already formed in the previous stage. [40]
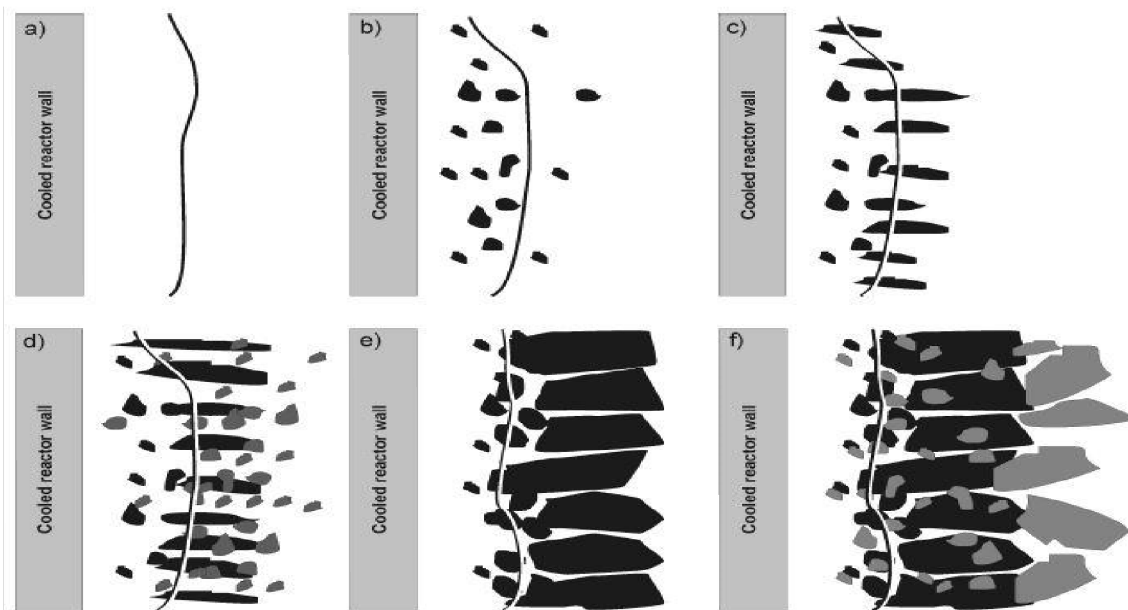
Figure 2.7 Different Stages in Freeze Lining growth [40]

When it prevents the corrosive liquid bath from coming into contact with the reactor wall, a freeze lining protects the wall, but it should also maintain stability under varying process parameters (composition and and typically near to or above the liquidus temperature. Because the thickness of the freeze-lining grows as the bath-lining interface temperature rises (while remaining below the liquidus temperature), obtaining a more protective freeze lining is possible regardless of closeness of the interface temperature to the bath temperature. [40]

According to the material's temperature distribution at the reactor wall, a glass layer develops. This implies that once the temperature rises, such a freeze lining will quickly vanish. Whereas Large crystals in an interface layer are not only dependent on the temperature distribution. The crystals have a different composition from the bath and are in equilibrium with it in a temperature range around the desired bath temperature (the wider this range, the better). Due to the need for mass transfer to dissolve the crystals in the bath, this different composition can slow down the freeze lining's shrinkage. Hence, a stable freeze layer consists of large crystals at interface layer. [40]

For a protective freeze lining, Campforts [40,38] recommended the following operational requirements: quick formation and sufficient stability in response to varying heat input and bath composition. They concluded that the establishment of an initial layer dominated by the existence of interlocking crystals combined with the subsequent production of a high-melting crystalline layer at the bath-freeze-lining interface can satisfy these requirements. The latter must be in equilibrium with the slag bath and have a sufficient compositional difference from the bath. While the low-melting phases bind the high-melting phases to the refractory, the high-melting phases shield it from corrosion. [41]

Following is explained the different Interface temperature phenomena in the formation of freeze linings [42] [43]:

$T_f < T_g$: In systems with slow crystallization kinetics and high glass transition temperatures, the interface temperature may be lower than the glass transition temperature. In that scenario, the interface layer is either glass- or microcrystalline-based.

$T_g < T_f < T_{liquidus}$: In this case, a subliquidus layer forms, which, causes continued crystallization toward the interface without attachment and redissolution back into the bath. However, there is no clear lining growth. As a result, the interface temperature is lower than the bulk bath's liquidus. This state will develop in systems with relatively slow mass transfer rates, which are prevalent in baths with little agitation or greater viscosity liquids. Focusing on the microstructure further clarifies that the interface layer's microstructure can be open or closed with respect to mass exchange with the liquid bath.

$T_f = T_{liquidus}$: The primary-phase crystals can form a strong primary-phase-sealing layer in which the interface temperature is equal to the liquidus temperature if relatively quick mass transfer from the bulk to the interface takes place. Systems with "fluid" liquids or intense bath convection could both provide the necessary high mass transfer rate.

$T_f > T_{liquidus}$: This scenario is consistent with a classic hot-face refractory design. As a result, they are more stable than the equilibrium primary phase of the bath materials because the high-melting refractory components are in direct contact with the liquid bath or can form solid phases with higher concentrations

of these high-melting elements. The refractory, however, can be continually consumed by slow erosion and dissolution as well as continuous mass transfer from the refractory. But even so, this procedure can take a while and provides long-term furnace integrity.

According to Crivits [5], the concentration and temperature profiles close to the reaction interface can theoretically be used to identify the rate-limiting step. The group of layers indicated by Crivits [44], which is depicted in **Table 2.3**, would come from the presence of the subliquidus layer and consideration of many alternatives. The categories put forth by Crivits [44] consider the possibility that the open crystalline layer could change into a sealed crystalline layer with prolonged exposure, as is typical in industrial applications. For industrial design applications, Tf=Tsolidus yields the maximum heat flow rate through the bath to interface and, consequently, through the wall and freeze lining.

Table 2-3: Various layers in freeze linings with their details [44]

nr	Name	Microstructural characteristics	Formation aspects
1	Quenched layer	Only glass phase (uniform and identical to bulk liquid)	High initial cooling rate remains below T_g
2	Devitrified quenched layer	Fine-precipitated crystalline solids in matrix of glass phase	Initially formed as glass, fine crystallites precipitated later
3	Closed crystalline layer	Mostly crystalline solids with residual liquid between crystals; Crystal dimensions increase further away from cold probe	Crystals precipitated directly from liquid, which was above T_g; no exchange of material with bulk liquid
4	Open crystalline layer	Large, widely spaced crystals with significant amount of liquid within open liquid channels	Open channels facilitate mass transfer with bulk liquid; liquid composition varies with distance from interface
5	Sealing layer	Consists solely of primary-phase crystals or other phases that are stable at the interface temperature	Theoretically formed at steady-state and chemical equilibrium
6	Subliquidus boundary layer	Intermediate layer between stagnant deposit and liquid bath	Temperature below $T_{liquidus}$ so that phases can precipitate
7	Entrained bulk bath liquid	Similar to the glass layer but located at the bath side of the freeze lining	Quenched after experiment, when probe is removed from bath

2.8. Effect of varying parameters on freeze lining formed by lab scale nonferrous slags

In the literature, both resistance furnaces [45],[46] and induction furnaces [6][47] have been used up to 1400 °C for lab scale investigations of freeze linings.

Sample rotation has been studied to see the effect of bath agitation on the thickness of the freeze linings in a slag system CaO-SiO2-FeO-ZnO-MgO-Al$_2$O$_3$, but it was found that there was no effect on the thickness although rotation increases the convection, but changes were noticed in the microstructure of these freeze linings by varying the rotational speed. [6]

The selection of the coolant for probe is done based on Heat transfer properties and safety reasons. Water is widely used as a coolant due to efficient heat transfer which leads to less flow rate requirements as compared to gas coolant. But it can lead to catastrophic failure if water somehow comes in contact with the molten slag bath [48]. Also, it was found out that cooling with water is too strong in comparison with the heat input from the slag bath due to which it was extremely difficult to reproduce an equilibrium thickness of freeze lining. So, it is recommended to work with a less insensitive cooling probe such as gas cooled probe. [6]

Both grade 316 stainless steel [47] and copper [46] have been used as a probe material. Copper is often used for the the various rigorous cooler designs. Stainless Steel has on the other hand a higher melting point as compared to copper which makes steel a safer substitute of copper.

Thermocouples must be selected according to their application. Such as, with proper temperature ranges and their exposure to a varying chemical environment. They are responsible for correct readings of energy input and output which helps in determining the valid results and analysis.

After the experiment is finished, the freeze lining can either be left in the furnace to cool down or it can be quenched in either water [45],[47] or nitrogen gas atmosphere [46] in order to stop any further microstructural or phase changes that can further occur in the sample.

2.8.1.   Change in Rotation Speed (RPM)

M. Campforts et al. [6] investigated the effect of molten slag bath agitation via crucible rotation on the formation of freeze linings in a Al2O3-CaO-FeO-MgO-SiO2-ZnO slag but there was no considerable effect noticed. After that, Fallah-Mehrjadi et al. [49] analyzed the effect of crucible rotation for a Cu-Fe-Si-Al-O slag and he was able to find out interesting results through increased heat convection via increase in Crucible RPM which includes:

- Change in composition and morphology of phases formed.
- Partial formation of Sealing layer.

Also, he found out that the increase in RPM increase the bath/freeze lining interface temperature closer to the liquidus temperature and the solid layer close to interface became denser.

As the RPM increases, shear thinning of slag occurs which means a decrease in the viscosity, [50] due to which there is fast crystallization of primary phase resulting in the formation of a stable primary phase sealing layer.[51]

2.8.2. Dynamic change in Slag Composition

S. Van Winkel [52] studied the effect of varying bath composition on the microstructure of freeze linings in the zinc fuming process. In this study, the author used ZnO and PbO additions and studied the effect of these additions on freeze lining formed after classifying 6 zones of freeze linings. In Zone 1,2,3 and 4 which are near to probe, there was no effect on the freeze linings because there was no Zn or Pb in those zones found out. Pb was only found out in the amorphous phase and the Zn was only present mainly in spinel and amorphous phase in the zones 5 and 6 which were close to the hot slag bath.

Crivits [53] studied the freeze lining evolution while changing the slag bath composition from one primary phase field to another. In the experiment, vertical tube thermaix furnace was used to melt the slags with different bath compositions as seen in **Table 2.4** at temperature of 1150°C and N2 gas flow rate of 2000 l/h. Three different slags were considered which included 2 with Olivine primary phase field and 1 with Wollastonite primary phase field.

Table 2-4: Various layers in freeze linings with their details [53]

Slag Name	SiO2	FeO	Fe2O3	CaO	Primary Phase
S1	41.6	48.8	0.4	9.3	Olivine
S2A	32.5	53.1	1.1	13.4	Olivine
S2C	40.9	39.3	0.2	19.6	Wollastonite

Transition of S1 slag into S2A slag was studied, which resulted in partial dissolution of pyroxene by freeze lining formation of S2A slag just before the original interface of both freeze linings where the second freeze lining starts to form, which resulted in the only presence of olivine with liquid right after the original interface towards the molten bath. Through this result it was concluded that there is limited dissolution of freeze lining in case of transition in same primary phase field slags. Moreover, transition of S1 into S2C slag was also investigated which resulted in complete dissolution of first freeze lining that was formed for S1 slag at the original interface of both freeze lining where second freeze lining starts to form. There was complete breakage of microstructure at the interface. From this result, it was interpreted that in case of transition in different primary phase field slags, there is complete dissolution of first formed freeze lining. In case of different primary phase field, the second form freeze lining was in contact with the already(first) formed freeze lining at some points and at some points it was not physically in contact which was proved via microstructure as well. From this fact, it was concluded that transition within different primary phase field freeze linings can have both positive and negative outcome in terms of stability. As there is no physical

contact, that means there is not enough physical strength and during industrial working condition the freeze lining can break easily with any physical force acted upon the furnace. On the other hand, it was also a positive thing that in case of erosion from slag bath the layer formed on the top will be affected immediately and because of less physical contact with the first formed freeze lining, there won't be much of chemical reaction occurring between both layers and the top layer will sacrifice itself in process of saving the already formed freeze lining that is S1 in this case. Both the transitions including S1 to S2A and S2 to S2C slag can be seen in the **Figure 2.8**.
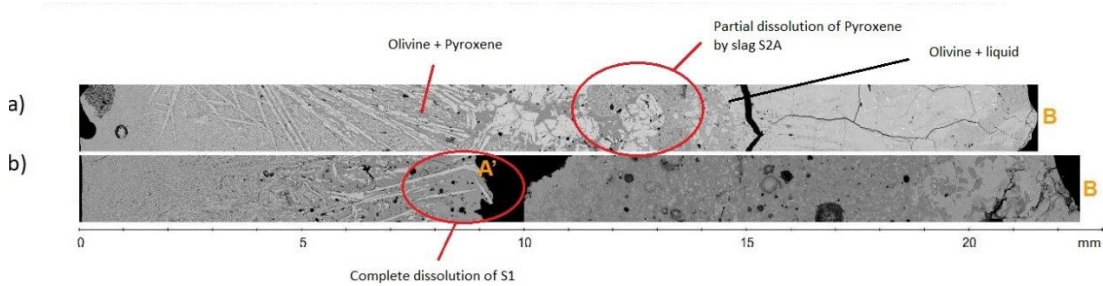
Figure 2.8 *a) Freeze lining S1 to Freeze lining S2A (both for 120 min. formation time), b) Freeze lining S1 to Freeze lining S2C (both for 120 min. formation time) [53]*

2.9.3. Effect of change in viscosity

A slag with roughly 15 wt.% SiO_2 was compared to a slag with a smaller proportion 9 wt.% percent SiO_2 by Fallah-Mehrjardi. [43] The later slag will have less viscosity than the former since slags' silica content has a significant impact on it. The freeze lining had reached a steady-state thickness in the lower viscosity system, according to the precise temperature readings. The freeze lining in the lower viscosity system took less time to attain its steady-state thickness, according to the precise temperature readings. The interface temperature was at the bath's liquidus temperature, and the deposit's microstructure clearly featured a dense-sealing layer made up of the primary phase. The primary phase's existence at the interface proves that there was no nucleation barrier preventing the primary phase from crystallizing on the solid-phase surfaces that were already there. On the other hand, the higher silica slag forms an open structure with a low solid fraction, and the more viscous the slag, the lower the interface temperature. [54]

Crivits [55] attempted to explain their findings as well as those from Fallah-Mehrjardi [43], who also considered slags with low viscosities (about 9 wt percent SiO_2) and intermediate viscosities (around 15 wt percent SiO_2). They provided an explanation for all these findings using the Fallah-Mehrjardi [43] mechanism in tandem with the inverse dependency of mass diffusivity on viscosity:

- It is possible for the sub liquidous boundary layer thickness in low-viscosity systems to become too thin, which would make it difficult to restore local equilibrium and would lead to additional expansion of the freeze lining.

- While crystals may form and redissolve in the boundary layer in systems with intermediate viscosities, there may not be a net change in the thickness of the freeze-lining because mass difusion toward the crystals inside the boundary layer may be sufficient to reach local equilibrium.

- Mass difusion to the crystals in the sub liquidous area is slow in extremely viscous slag systems, preventing the attainment of a local equilibrium in this layer and causing the freeze lining to thicken.

2.9.   Sub-liquidus boundary layer

It was widely recognized previously that the interface temperature between bulk bath and the deposit is the liquidus of the bulk bath material [56] [57] but more recent research work has proved that it can be even lower than liquidus temperature as well i.e., between liquidus and solidus temperature. This has been found out using a phenomenon including detached crystals on which nucleation and growth of solid occurs in a "sub liquidous layer" because of movement of fluid material in the direction of the stagnant deposit interface and then these detached crystals again get dissolved into the liquid bath as they are washed away by turbulent eddies as shown in **Figure 2.9**.

The recent lab investigations have also shown that the phases formed at the stagnant deposit/ bath interface are not necessarily the primary phase. [42]

According to the concept of "sub liquidous layer", it is explained that crystal growth can occur on detached crystals moving in the mobile multi-phase solid-liquid layers, i.e., subliquidous layer as well other than the stagnant deposit interface. The convective flows transport all the precipitated detached crystals far away from the deposit interface toward the slag bulk liquid and transport the material towards the deposit interface. Consequently, the precipitated crystals get dissolved into the molten bath because of high temperature of molten bath. [42]
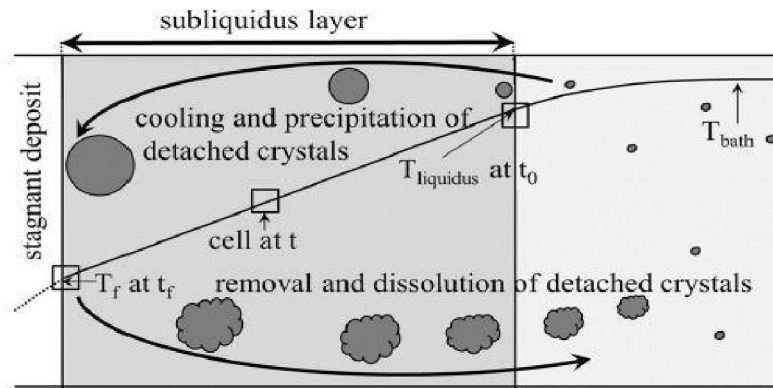
Figure 2.9 *Schematics of mechanism happening in the subliquidus layer at the bath/deposit interface [42]*

In short words, latest findings suggest that nucleation and growth of the solid phase is prominent in a subliquidus layer in the form of fluid phase (mushy zone, that is mobile multiphase solid-liquid layers) on the detached crystals in the close vicinity to the freeze lining deposit surface. Moreover, the bath/deposit interface temperature is also expected to be between the solidus and the liquidus of the molten bath. Further research on this model can play a vital role in decreasing the energy input, operating temperature and the operational costs. [58]

Nagraj [59] investigated the temperature of bath/freeze lining interface based on rheology of the slag. Throughout the zinc fuming process, the slag bath's composition varies continuously, altering the interface between the bath and freeze lining. So, three slags with various Zn contents were chosen. Industrial slag from Metallo Belgium's secondary copper smelter was employed as Slag A in that study. The relative content of the remaining slag components was kept constant while the ZnO content was changed to create Slag B and Slag C, which have ZnO contents of 8 weight percent and 11 weight percent, respectively, from Slag A.

According to investigations of viscosity, it was found that the Zn concentration has no effect on the critical temperature at which the copper slag quickly transitions from a liquid-like phase to a solid-like regime, which is 1080°C. The microscopic examination of the equilibrium quenching test samples revealed that the solid fraction at the critical viscosity temperature was 41+/- 4.8 percent when the crystals agglomerated. According to the microscopic analysis of the freeze lining samples, the liquid slag's hydrodynamics and the interactions between the crystals and the liquid slag at the interface determine the solid percentage at the hot face. The temperature at the bath/freeze lining interface, which is below the critical viscosity temperature, is in the range of 1035–1070°C. At 0, 30, 60, and 90 rpm, respectively, the average solid fraction at the hot face of the freeze lining was 58 +/-10.1 percent, 59 +/-5.5 percent, +/-61 +/- 4.9 percent, and 67 +/-3.9 percent. [59]

2.11. Summary

Freeze linings has been an extremely interested topic of research to prolong the life of pyrometallurgical furnace. Till today freeze linings are investigated in numerous types of furnaces. Various cooling designs and materials have been investigated. Freeze linings can be beneficial for ISASMELT furnace to avoid the wear and tear of lance material and reactor container walls. Out of all the experimental techniques being used to investigate the microstructure of slag solidification, cooled probe technique is much better.

It has been found out, formation of freeze lining is supported by thermal balance among heat output through the cooled furnace wall Q_{wall}, heat input from the superheated Slag bath Q_{bath} and the latent heat of fusion at the hot face of freeze lining Q_{fusion}. The temperature gradient and solidification rates are continuously changing during freeze lining formations which results number of zones being formed referring to different microstructures in a freeze lining. The ratio of temperature gradient and solidification rate determines the growth morphology.

Research including effect of varying parameter on formation of freeze lining through nonferrous slags shows, change in rotational speed of crucible containing molten slag bath can cause change in composition and morphology of phases formed. Increase in RPM increase the bath/freeze lining interface temperature closer to the liquidus temperature which make solid layer close to the interface denser. Research on dynamic change in slag bath composition shows only the zones of freeze linings near the molten bath were affected. In another research where change in slag bath composition was done by changing from primary phase field to another. It was concluded, in case of same primary phase field slags transition only a limited dissolution occurred in the already formed freeze lining whereas, in case of different primary phase field transition, complete dissolution of already formed freeze lining occurred. In both the cases, after transition of slag bath composition new freeze lining was formed on top of surface of previously formed freeze lining.

Chapter 3

3. Materials and Methodology

The slag system chosen in this thesis is the SiO_2-FeO-CaO-Al_2O_3 system. The slag compositions are selected to be in either the melilite or spinel primary phase field, which are important phase fields for the slags applied in the recycling processes at Umicore.

FactSage software is being used to plot the ternary phase diagram and to perform the equilibria calculations. Computation and manipulation modules make up the FactSage computer package, which enables access to manipulation of solution databases and compounds. Chemical and physical metallurgists, corrosion engineers, chemical engineers, etc. may find tables, graphs, and figures produced by its extensive range of thermochemical computations useful. With a variety of axes, it can compute and plot binary, ternary, and multicomponent phase diagrams. When thermochemical tables were calculated and printed using mainframe computers forty years ago, the turnaround time was measured in hours. With today's personal computers, phase diagrams may be calculated and plotted in a matter of seconds.

With the help of composition selected for both primary phase fields from FactSage calculations, freeze linings are formed in both primary phase fields for 30 min. and 3 hours' time durations to see at which time duration, freeze lining seemed to have achieved steady state thickness and then transition from one primary phase field freeze lining to the other primary phase field freeze lining i.e., formation of spinel primary phase field freeze lining and then inserting it into molten bath of melilite primary phase field slag composition and vice versa is analyzed at selected time duration which is 3 hours to see what happen to the microstructure and morphology of freeze lining.

3.1. FactSage calculations and slag preparation

The SiO_2-FeO-CaO-Al_2O_3 system phase diagram at a fixed Al_2O_3 content of 10 wt% plotted with FactSage at 1160 °C can be seen in **Figure 3.1**. This diagram is used to select slag compositions with respectively melilite and spinel as target phases. 'Calculate' module with FactPS and FToxid databases is used. The aim is to find spinel and melilite primary phase fields at same temperature. Then random composition points in both primary phase fields is selected and compositions at both points is calculated manually. Once composition for both primary phase fields is known, Equilib function is used to perform equilibrium calculations which helped plot the solidification curves indicating which phase is precipitating first while temperature is decreasing below liquidous temperature and how much a specific primary phase is precipitating before the precipitation of second phase at the normal partial pressure of oxygen 10^{-12} ppm. This is important to know so that a freeze lining formed with a specific primary phase field has enough

amount of primary phase crystals present in its microstructure. Furthermore, it also indicated the order of precipitation of different phases as the temperature drops below the liquidous temperature. As seen in **Figure 3.2** and **Figure 3.3**, It is found out, at 1160 °C, with the selected composition for spinel primary phase field freeze lining, precipitation of spinel crystals accounts for 3.7wt% of total mass before secondary phase starts to precipitate. Whereas precipitation of melilite crystals accounts for 13wt% of total mass before secondary phase starts to precipitate. **Table 3.1** show the selected slag compositions.

It was also confirmed by doing equilibria calculations on FactSage by keeping total composition as a fixed unit of 100 grams using same composition as depicted by ternary phase diagram to see how much primary phase is going to form before the precipitation of secondary phase. It was found out, at the liquidus temperature 1160 °C with the composition shown in **Table 3.1**, 3.7 grams of Spinel will form before the first precipitation of secondary phase and 13 grams of Melilite is going to form before the secondary phase precipitation at that composition as depicted in **Figure 3.2** and **3.3** respectively.

Table 3-1: *Selected slag composition within spinel and melilite primary phase fields.*

Components	Slag Composition	
	Spinel Primary Phase Field (S1) wt %	**Melilite Primary Phase Field (S2) wt %**
SiO_2	31.5	31.5
FeO	44.7	36.6
CaO	13.8	21.9
Al_2O_3	10.0	10.0
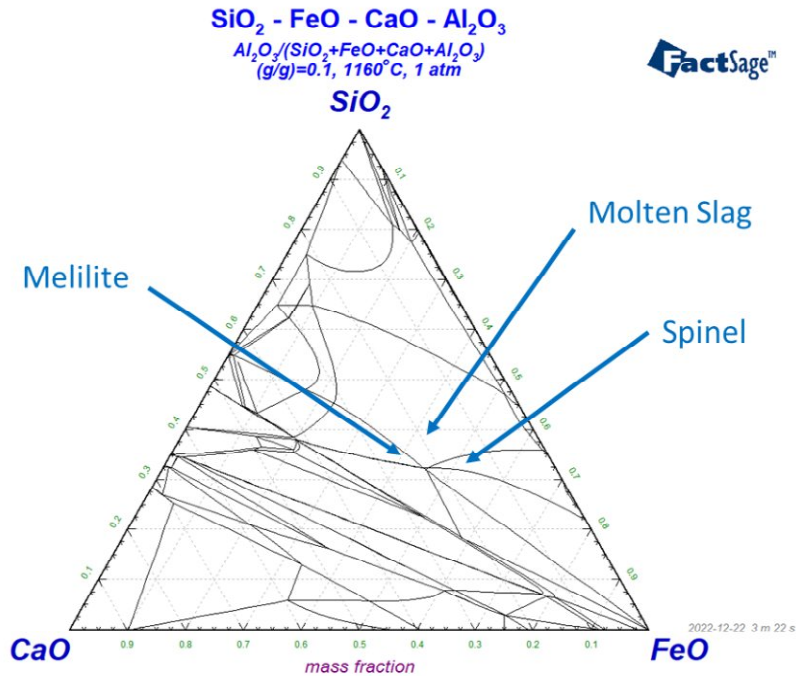
Figure 3.1: *Phase diagram for the SiO2-FeO-CaO-Al2O3 system with Al2O3 content fixed at 10% at 1160 °C showing the potential zones for the formation of Spinel and Melilite phases and the zone where melting of this slag system occurs.*
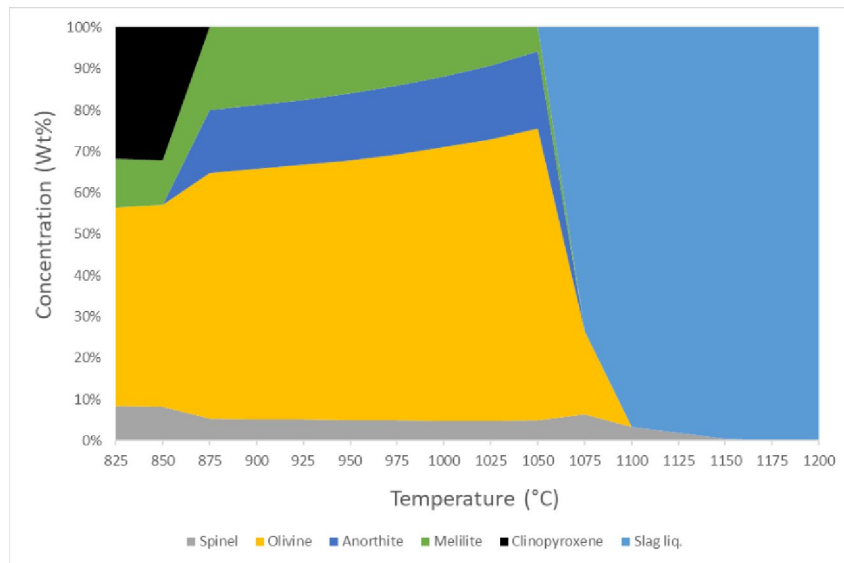
Figure 3.2 *: Equilibrium cooling curves showing the formation of 3.7wt% of spinel when secondary phase starts to form in S1 slag.*
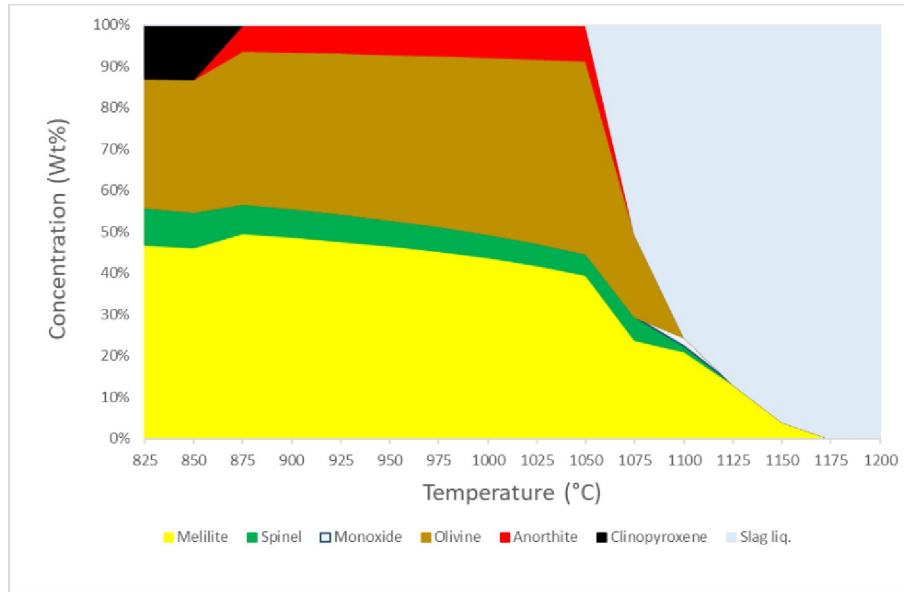
Figure 3.3: *Equilibrium Cooling curves showing the formation of 13wt% of Melilite when secondary phase starts to form is S2 slag.*

Upon solidification of Slag S1, spinel is the primary phase forming at 1160 °C as seen in **Figure 3.2**. At 1091 °C, olivine and anorthite starts to precipitate out. The fraction of spinel, olivine and anorthite starts to increase simultaneously. At 1071 °C, melilite starts to form and the last portion of molten slag gets solidified. Until 867 °C, melilite increases gradually while Anorthite and Olivine decreases and then Clinopyroxene starts to precipitate out. After the formation of clinopyroxene, spinel and melilite continue to increase while the other phases decrease in the amount with decreasing temperature.

The first phase upon solidification at 1160°C for the slag S2 is melilite as seen in **Figure 3.3**. At 1124.5 °C, spinel begins to form. The fraction of melilite and spinel begins to increase simultaneously. At 1121 °C, monoxide begins to form, and its amount increases until 1078 °C and then gets dissolved back into the molten slag. Also, at the same temperature, olivine begins to precipitate. At 1071 °C, anorthite begins to form and all the molten slag gets solidified. Anorthite increases simultaneously with already formed phases. At 867 °C, clinopyroxene starts to precipitate and the anorthite amount reaches 0. Afterwards, the amount of clinopyroxene and olivine decreases with decreasing temperature, while spinel and melilite phase further increases in fraction.

To perform the experiment; SiO_2 (99.5% pure) and Fe_2O_3 (98% pure) from the supplier named 'Thermo Fisher (Kandel) GMBH', CaO (96% pure) and Al_2O_3 (99% pure) from the supplier named 'Acros Organics NV) and Fe ($\geq$ 99% pure) from the supplier named 'Merck Life Science BV) are used to prepare the slag mixture. The volume of Al_2O_3 crucible being used can safely contain 600 g of slag mixture by leaving some space at the top region to have allowance for the vigorous splashing happening in molten slag bath in the heated furnace. Accordingly, the wt% of all the components in both S1 and S2 slags are multiplied by the

31

factor of 6 to get the slag mixture with overall mass of 600 g which can be seen in **Table 3.2**. Moreover, Fe and Fe2O3 is added in the slag mixture by calculating their amount according to amount of FeO. Firstly, all the components are mixed except Fe before every experiment in a turbula mixture equipment. Fe is added afterwards and mixed manually just before the experiment because of its high tendency of reacting with oxygen to form oxide.

Table 3-2: *Quantities of all components of slag mixture used in all the experiments.*

	SiO_2 (g)	Al_2O_3 (g)	CaO (g)	Fe	Fe2O3
S1 slag mixture	189.00	60.00	82.80	69.42	198.66
S2 slag mixture	189.00	60.00	131.40	56.76	162.84

3.2. Experimental procedure and setup

For every experiment, 600g of slag is filled in an alumina (Al_2O_3) crucible and is melted at 1180 °C. 20 °C more than targeted temperature 1160 °C to consider the factor of super-heating, because when cooled probe is inserted, it can drop down the slag bath temperature in a vertical tube Thermaix furnace as shown in **Figure 3.5**. Vertical tube thermaix furnace is a resistance furnace, which consists of heating elements (resistors) located at inside wall of the furnace and the workpiece is heated mainly via radiation and convection. This furnace is also made gas tight while operating with Argon (Ar) flushing. According to the calibration of furnace, an actual slag bath temperature of 1180 °C is achieved when the furnace temperature is set to 1277 °C. The heating rate of the furnace is 7 °C/min until 1000 °C followed by 4 °C/min until 1150 °C, and 2 °C/min from 1150 °C till 1250 °C. After that, it is only 1 °C/min to reach the 1277 °C target temperature. After reaching 1277 °C, the temperature is kept on hold for 2 hours to complete homogenization of the slag. Argon (Ar) flushing helped reaching an inert atmosphere. Then, a N_2 cooled stainless steel probe is submerged into the molten slag bath. A Cross-sectional image of the vertical Thermaix furnace and the stainless-steel probe can be seen in **Figure 3.4 (a)** and **Figure 3.4 (b)** respectively.
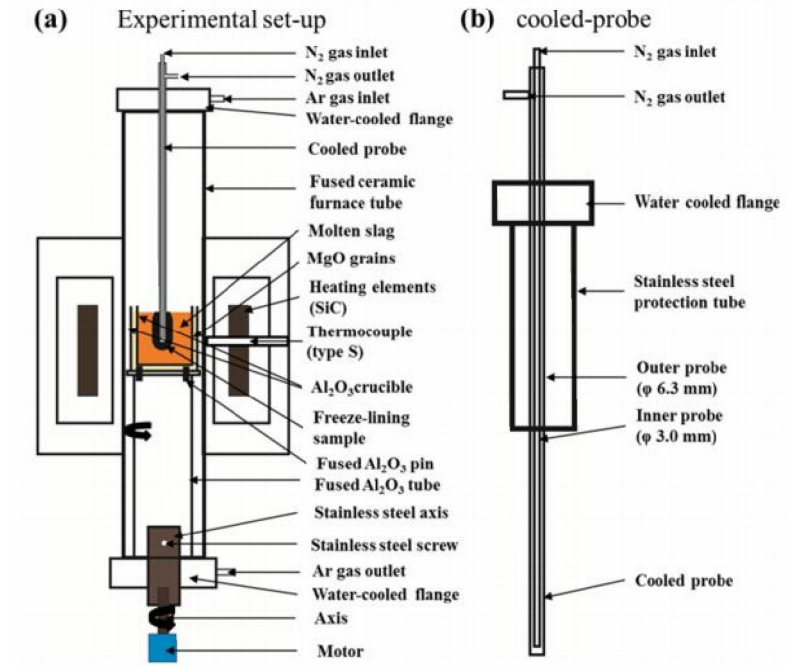
Figure 3.4: (a) Cross Section of the vertical Thermaix furnace (b) N2-cooled stainless-steel probe (courtesy MTM, KU Leuven)

When the N_2-cooled stainless steel probe is submerged in the molten bath from the top of furnace, the slag gets solidified onto the cooled surface because of the thermal gradient achieved. Afterwards, the probe is taken out with a freeze lining formed and quenched in water at room temperature. After all the steps of experiments are done, furnace is set to cool down with the cooling rate of 5°C/min.

The number of experiments performed during this research with details can be seen in **Table 3.3**. For the first 4 experiments, individual freeze linings are formed in a specific primary phase field (S1 and S2) after submerging the probe in the molten bath for different submergence times followed by taking out the probe with freeze lining from the furnace to quench it in water at room temperature. Experiment 3 and 4 were performed by Gaelle Butin who is my daily supervisor for this thesis. As far as Experiments 5 and 6 are concerned, they involve a transition of slag bath to investigate the microstructure of the formed transient freeze linings. In both experiments, first a freeze lining is formed in a specific primary phase field slag followed by quenching and allowing it to cool down. Afterwards, it is again submerged into a slag with another primary phase field slag to form the freeze lining on top of previously formed freeze lining to investigate the effect of change in slag bath. In **Figure 3.6(a)**, freeze lining formed after quenching in one of the transient phase freeze lining formation experiments is seen and in **Figure 3.6(b)**, freeze lining formed after quenching in one of the single primary phase steady state freeze lining formation experiments can be seen.

Figure 3.5. *Vertical thermaix furnace setup (courtesy MTM, KU Leuven)*

Figure 3.6: (a) Spinel to melilite transition freeze lining (b) Spinel steady state freeze lining (3hrs.)

Table 3-3: *Details of experimental plan.*

Experiment No.	Freeze lining label	Description	Submergence time	N_2 flow
1	FL1	S1 freeze lining	30 min.	~35 liter/h
2	FL2	S2 freeze lining	30 min.	~35 liter/h
3	FL3	S1 freeze lining (Gaelle Butin's work)	3 hrs.	~35 liter/h
4	FL4	S2 freeze lining (Gaelle Butin's work)	3 hrs.	~35 liter/h
5	FL5	Formation of new S1 freeze lining followed by its submergence into S2 molten bath	3 hrs. for both the initial formation of S1 freeze lining and the submergence of S1 freeze lining	~35 liter/h for S1 freeze lining formation and ~38 liter/h for the submergence of S1 freeze lining
6	FL6	Formation of new S2 freeze lining followed by its submergence into S1 molten bath.	3 hrs. for both the initial formation of S2 freeze lining and the submergence of S2 freeze lining	~38.5 liter/h for S2 freeze lining formation and ~34 liter/h for the submergence of S2 freeze lining

3.3. Sample preparation

After the end of all the experiments, to investigate the microstructure of freeze linings, the long probe is cut down from nearby region of freeze lining. In some cases, the freeze linings itself split into pieces while cutting the probe but sometimes it remained intact. Then the freeze linings are embedded into mixture of epoxy resin and a hardener (ratio of epoxy resin to hardener is 15:2). After this the embedded samples are kept in a vacuum chamber to extract all the gas bubbles from the sample. The resin and a hardener mixture

take around 24 hours for complete hardening. In the next step, freeze linings which remained intact with the probe, they are cut right through them to expose the cross section. In other case, the cross section was already accessible. Exposed cross section surface of embedded freeze linings is grinded via Silicon carbide papers ranging from P320, P800, P1200 and P4000 to produce a cross section. Then the microstructure is analyzed under an optical microscope and when microstructure is clear enough then the samples are polished with diamond suspension. Afterwards the grinded and polished cross-section surface of samples are carbon coated by using a turbomolecular pumped coater Q 150 TE equipment. For the samples FL3 and FL4, a platinum coating is instead applied. The embedded polished samples of FL1, FL2, FL5 and FL6 can be seen in **Figure 3.7**.
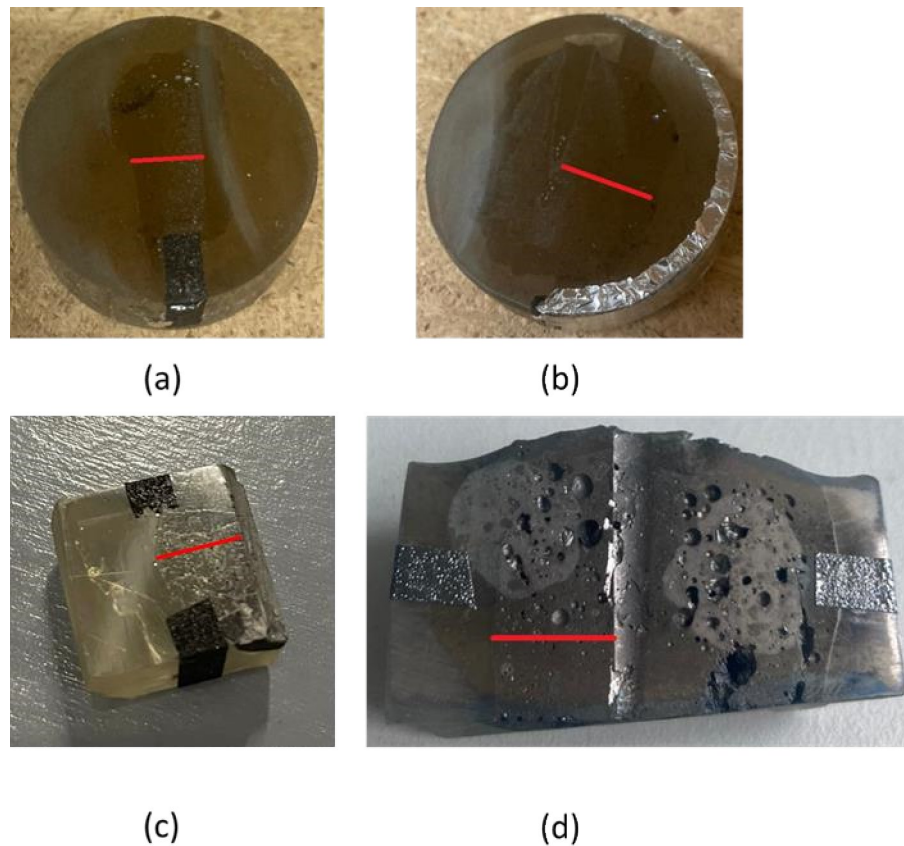
Figure 3.7: The embedded polished samples of freeze linings.(a) Spinel primary phase freeze lining (30 min. formation time), (b) Melilite primary phase freeze lining (30 min. formation time), (c) Melilite to Spinel transition freeze lining (3 hours formation time for both the freeze linings), (d) Spinel to melilite transition freeze lining (3 hours formation time for both the freeze linings) (red marked line shows the area which is analyzed through SEM-BSE, SEM-EDAX and WDS-EPMA.

The reason for embedding, grinding, polishing and carbon/platinum coating is to analyze the samples under Scanning electron microscopy (SEM) using an XL30 FEG equipment. Back scattered electron (BSE) diffraction images are collected at 15 kV acceleration voltage to analyze the microstructure of the sample. Electron dispersive Xray spectroscopy (EDAX) is used to find the overall global compositions at certain

distances over the whole profile of freeze lining starting from the probe till molten bath. Also, it was used to find the composition of phases. Electron probe microanalyzer (EPMA) technique is also used to find the composition of the phases with following operating conditions: 15 kV acceleration voltage, $5\text{x}10^{-8}$ Ampere current, measuring time on peaks is 10 seconds and on the background is 5 seconds. Moreover, the standards for quantification used are, Si standard: Willemite, Fe & Al standard: Almandina garnet and Ca standard: Diopside. Electron backscatter diffraction (EBSD) analysis was also performed on FL4 freeze lining to confirm the identity of the melilite phase. All the samples are analyzed over the distance from the probe towards the molten bath around the central region of the freeze linings.

Chapter 4

4. Results and Discussion

This chapter consists of Back Scattered Electron (BSE) images attained through Field Emission Gun-Scanning Electron Microscopy (FEGSEM) of the freeze lining samples. Moreover, the global composition and composition of the individual phases present in the freeze linings are analyzed using Electron Dispersive Xray Spectroscopy (EDAX) and Electron Probe Microanalyzer (EPMA) techniques. All freeze linings are discussed in terms of their microstructure and thickness. FL5 and FL6 freeze linings are compared against the FL3 and FL4 freeze linings respectively with respect to the phases formed at certain distances from the probe and to the type of layers being formed and the crystal growth morphology in the freeze lining.

This chapter starts with presenting the microstructures of the freeze linings in sections 4.1 and 4.2, for which the following should be considered:

- The freeze linings formed in all the experiments have variable thickness from probe till molten bath. For instance, if we measure the thickness of any freeze lining at one specific point, most probably it won't be identical to the thickness measured for that freeze lining at another point.
- All SEM-BSE images showing the overall profile/thickness of freeze linings starting from probe till the slag bath are multiple images taken at 100x magnification and then stitched together to form one large image.
- The composition of the different phases around certain distances from the probe is determined by EPMA-WDS in FL1, FL2, FL3 and FL4 but for FL5 and FL6 EDAX was used. The obtained composition of phases was matched with the expected phases according to the equilibria calculations of FactSage and using an online mineralogy database [60].

4.1. Microstructural study of the freeze linings obtained in the spinel and melilite primary phase slags, with varying submergence times

In this paragraph, the freeze linings obtained from a single immersion step in the spinel or melilite primary phase slags will be studied. Two immersion times are performed for the two slags: 30 min and 3 h. The submergence time for the transient experiment will be selected based on the results of these experiments.

4.1.1. FL1: Freeze lining from slag S1 with spinel as primary phase, 30 minutes submergence time

FL1 freeze lining has 3 different layers (**Figure 4.1**). The overall thickness of the freeze lining is around 9 mm. The freeze lining is fully crystalline until around 5.5 mm from the probe. This is called the crystalline layer. Then, until around 7 mm, there is an open crystalline layer, where crystals are still intact with the crystalline layer but a significant amount of solidified amorphous slag is present in-between. Afterwards, an entrained slag bath layer is present until the end of the freeze lining containing widely spaced spinel and anorthite crystals. These crystals are detached from the crystalline and the open crystalline layer and are floating freely in the solidified amorphous slag present in-between. It is the molten slag bath which remained attached to the surface of the freeze lining while taking the probe out of furnace, and that solidified during the quenching of this freeze lining. A zoomed in image of this entrained slag bath layer is shown in **Figure 4.2**.

Figure 4.1: *SEM-BSE stitched image of FL1 after 30 minutes of submergence time. (1) Crystalline layer (2) Open crystalline layer (3) Entrained slag bath layer*

Figure 4.2: *Widely spaced and detached spinel and anorthite crystals in the open crystalline layer of FL1. An; Anorthite, Sp; Spinel, SM; Solidified Slag Matrix*

The phases formed in FL1 around 2, 5 and 6 mm from the probe and their respective average composition can be seen in **Figure 4.3** and **Table 4.1**. From **Figure 4.3a**, it is visible that the spinel phase is included in the anorthite phase, the anorthite phase is included in the olivine phase and the olivine phase is included in the melilite phase around 2mm distance from the probe. This means spinel is precipitated first followed by respectively the precipitation of anorthite, olivine and then melilite.
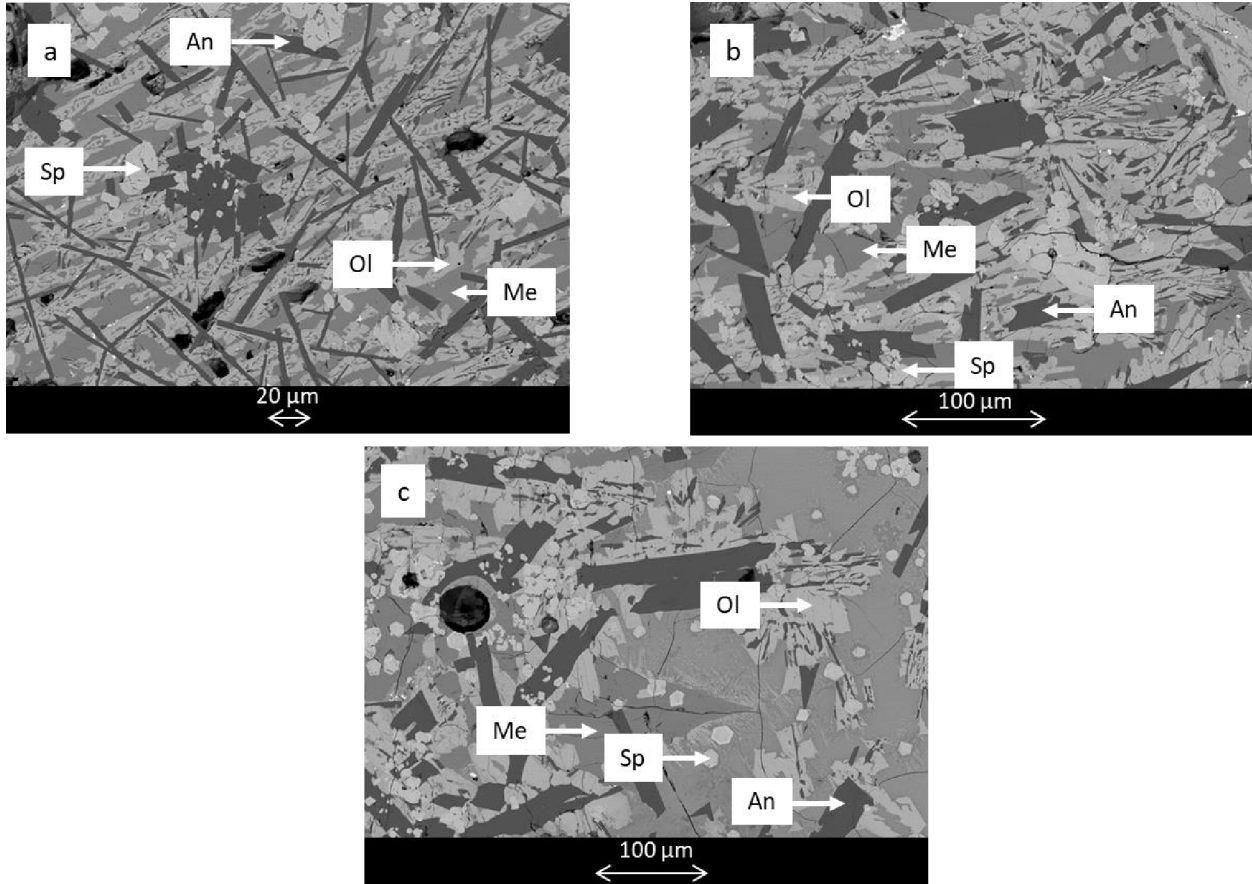
Figure 4.3: *BSE images of FL1 showing the presence of different phases at certain distances from the probe. (a) Around 2 mm distance (b) Around 5 mm distance (c) Around 6 mm distance. An; anorthite, Ol; olivine, Sp; spinel, Me; melilite*

Table 4-1: *Average composition of the phases formed in the freeze lining FL1 at specific distances from the probe.*

Distance from probe	Phases formed	Al_2O_3 (wt.%)	SiO_2 (wt.%)	CaO (wt.%)	FeO(wt.%)

Around 2 mm	**Spinel**	16.9 ± 1.6	0.6 ± 0.3	0.4 ± 0.1	82.0 ± 2.0
	Anorthite	33.9 ± 0.6	44.9 ± 0.3	19.6 ± 0.2	2.2 ± 0.3
	Olivine	0.7 ± 0.3	30.6 ± 0.1	7.3 ± 0.2	59.2 ± 0.7
	Melilite	8.0 ± 0.5	41.9 ± 1.7	20.0 ± 0.3	28.2 ± 0.4
Around 5 mm	**Spinel**	16.5 ± 1.4	0.1 ± 0.7	0.4 ± 0.3	82.1 ± 0.3
	Anorthite	33.3 ± 0.4	45.4 ± 0.2	19.4 ± 0.1	2.6 ± 0.2
	Olivine	0.1 ± 0.0	30.7 ± 0.2	6.2 ± 0.8	60.9 ± 1.0
	Melilite	7.5 ± 0.7	42.7 ± 0.4	21.4 ± 0.1	27.2 ± 0.3
Around 6 mm	**Spinel**	17.6 ± 0.9	3.5 ± 3.2	1.6 ± 1.5	77.2 ± 4.0
	Anorthite	32.7 ± 0.4	45.6 ± 0.4	19.4 ± 0.2	2.7 ± 0.5
	Olivine	-	31.1 ± 0.4	8.9 ± 2.5	58.1 ± 2.5
	Melilite	7.0 ± 0.4	41.2 ± 0.7	19.7 ± 0.4	30.7 ± 0.6

4.1.2. FL2: Freeze lining from slag S2 with melilite as primary phase, 30 minutes submergence time

FL2 freeze lining also consists of 3 layers **(Figure 4.4)**. The overall thickness of FL1 is around 16 mm. This freeze lining is fully crystalline until around 8 mm from the probe. Then, until around 9.5 mm, there is an open crystalline layer. Afterwards, an entrained slag bath layer is present which consists of widely spaced spinel and anorthite crystals with the presence of high amount of solidified amorphous slag in-between as was the case in FL1. After 4 mm distance from the probe, the melilite phase stopped precipitating.
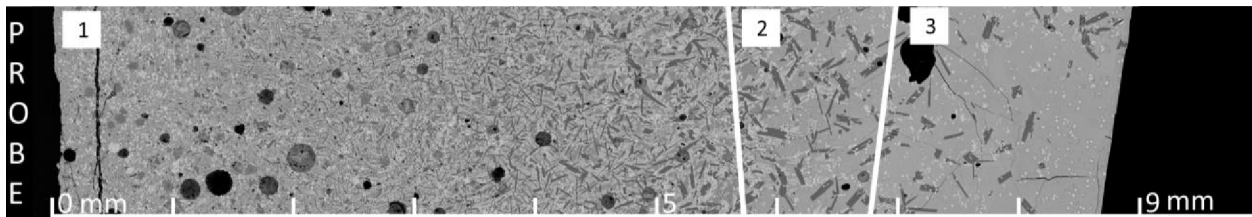

Figure 4.4: *SEM-BSE stitched image of FL2 after 30 minutes of submergence time. (1) Crystalline layer (2) Open crystalline layer (3) Entrained slag bath layer*
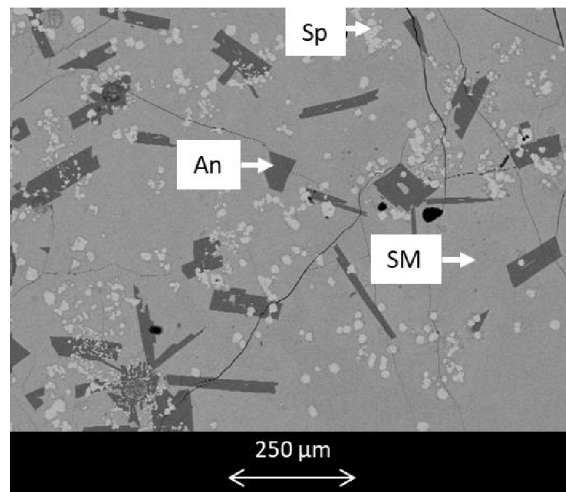
The phases formed and their respective average composition can be seen in **Figure 4.5** and **Table 4.2**. As seen in **Figure 4.5b**, the spinel phase is included in the anorthite phase, the anorthite phase is included in melilite phase and the melilite phase is included in the olivine phase. Hence, the order of crystallization here is spinel, anorthite, melilite and then olivine. Alunimum enriched spinel is also formed in this freeze lining which has higher amount of aluminum and decreased FeO content **(Table 4.2)** as compared to a normal spinel phase.

Figure 4.5: *BSE images of FL2 showing the presence of different phases at certain distances from the probe. (a) Around 1.15 mm distance (b) Around 4 mm distance (c) Around 7.5 mm distance. An; anorthite, Ol; olivine, Sp; spinel, Me; melilite, Al-Sp; Al$_2$O$_3$-enrcihed spinel, SM; Solidified slag matrix*

Table 4-2: *Average composition of the phases formed in the freeze lining FL2 at specific distances from the probe.*

Distance from probe	Phases formed	Al$_2$O$_3$ (wt.%)	SiO$_2$ (wt.%)	CaO (wt.%)	FeO(wt.%)

Around 1.15 mm	**Melilite**	8.9 ± 0.4	42.7 ± 0.7	22.1 ± 0.0	25.5 ± 0.3
	Anorthite	33.3 ± 0.9	44.9 ± 0.6	19.7 ± 0.2	2.1 ± 0.6
	Olivine	1.5 ± 1.0	31.0 ± 2.6	19.2 ± 2.0	46.4 ± 5.2
Around 4 mm	**Spinel**	15.7 ± 1.6	0.6 ± 0.4	0.6 ± 0.2	83.2 ± 1.5
	Anorthite	33.4 ± 0.1	44.8 ± 0.2	19.7 ± 0.1	2.3 ± 0.0
	Olivine	0.1 ± 0.0	32.3 ± 0.2	27.2 ± 0.3	38.5 ± 0.30
	Melilite	10.7 ± 1.2	41.1 ± 0.8	22.5 ± 0.2	24.4 ± 0.4
	Al_2O_3- enriched Spinel	51.8 ± 0.8	0.8 ± 0.6	0.6 ± 0.2	42.9 ± 0.1
Around 7.5 mm	**Spinel**	12.7 ± 0.2	0.2 ± 0.4	0.4 ± 0.0	86.8 ± 0.1
	Anorthite	34.1 ± 0.1	44.7 ± 0.1	19.0 ± 0.1	1.8 ± 0.3
	Olivine	0.6 ± 0.6	32.9 ± 0.5	27.0 ± 0.2	36.7 ± 0.8
	Solidified slag matrix	7.2 ± 0.1	35.0 ± 0.5	20.9 ± 0.9	36.9 ± 0.7

4.1.3. FL3: Freeze lining from slag S1 with spinel as primary phase, 3 hours submergence time

There are 3 different layers in the freeze lining FL3 as seen in **Figure 4.6**. The overall thickness of FL3 is around 16 mm. The crystalline layer is present until around 9.5 mm from the probe. Then, around 9.5-11 mm an open crystalline layer is present. Then, till the end of the freeze lining the entrained slag bath layer is present with the presence of widely space spinel and anorthite crystals. This layer looks glassy in appearance.
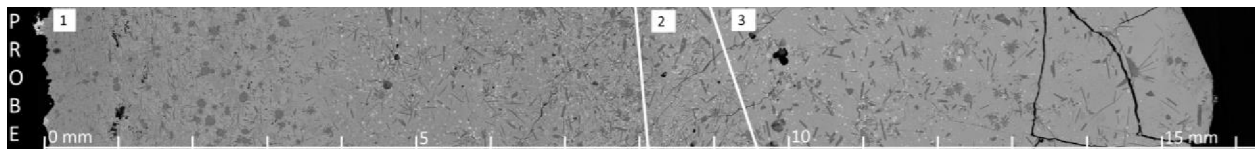
Figure 4.6: SEM-BSE stitched image of FL3 after 30 minutes of submergence time. (1) Crystalline layer (2) Open crystalline layer (3) Entrained slag bath layer

The phases formed can be seen in **Figure 4.7.** As seen in **Figure 4.7a**, the spinel phase is included in the melilite phase and, the anorthite phase precipitated together with the olivine phase. Hence, the order of crystallization is spinel and melilite followed by the eutectic growth of anorthite and olivine together.
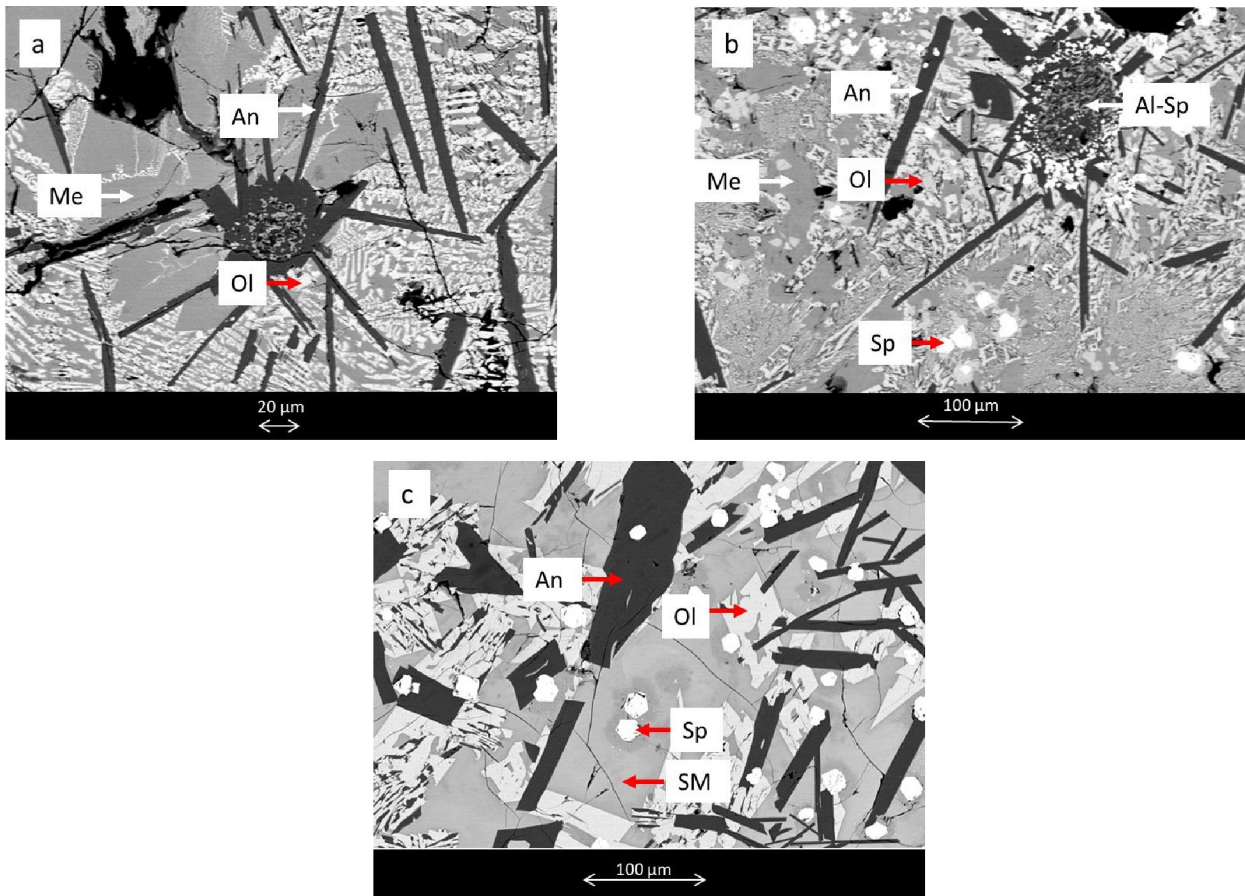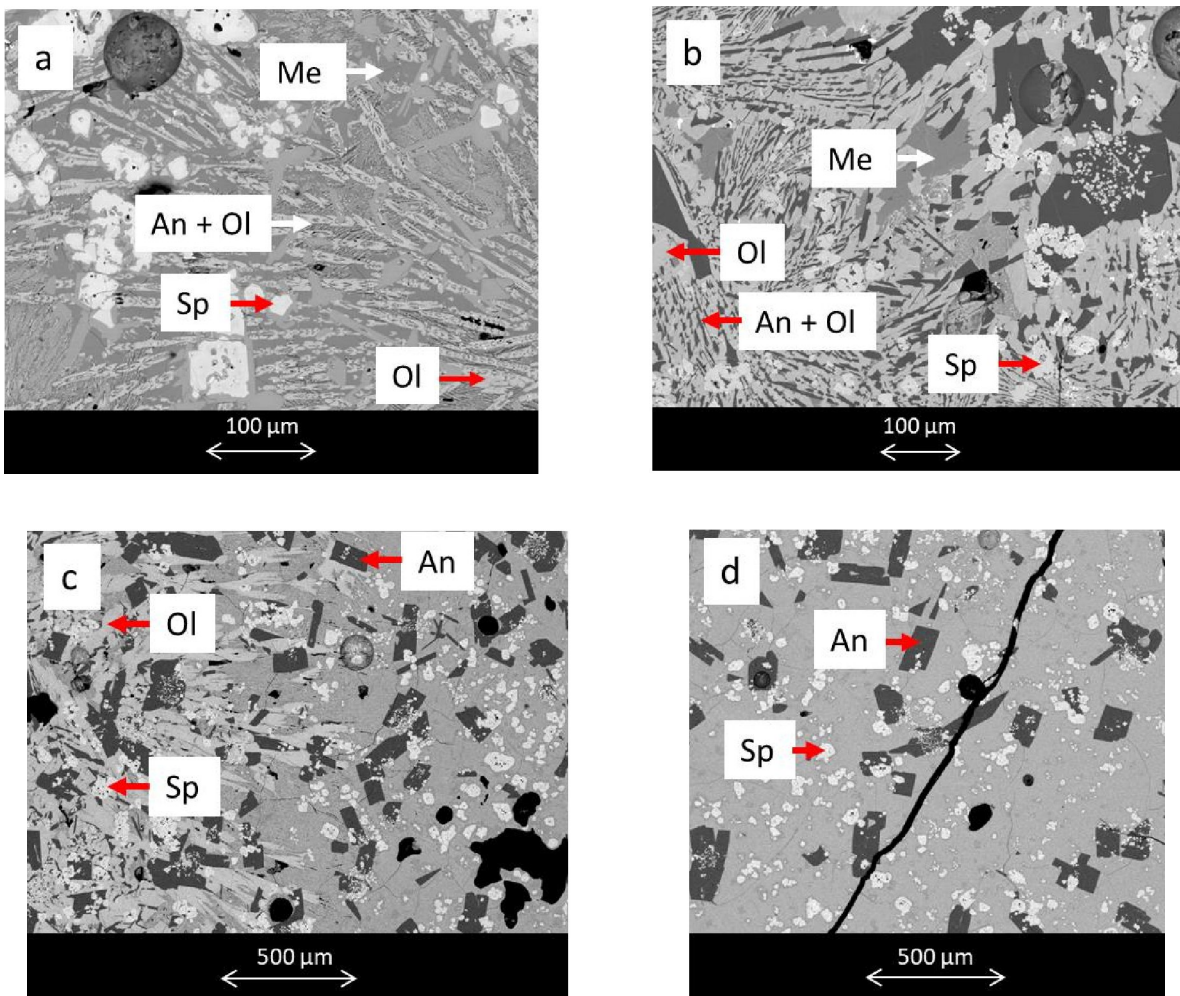

Figure 4.7: BSE images of FL3 showing the presence of different phases at certain distances from the probe. (a) Around 3 mm distance (b) Around 9 mm distance (c) Around 11 mm distance (d) Around 12 mm. An; anorthite, Ol; olivine, Sp; spinel, Me; melilite, An + Ol; anorthite + olivine growing together

The composition of solidified slag matrix at different distances from the probe in the open crystalline layer and entrained slag bath layer of the freeze lining formed in S1 slag composition for 3 hours (FL3) is almost similar to S1 whole slag composition as shown in **Table 4.3**.

Table 4-3: *Measured composition of the solidified slag matrix in FL3 at different points around 10-15 mm distance from the probe and the overall average composition.*

Distance from Probe (mm)	Al_2O_3 (wt.%)	SiO_2 (wt.%)	CaO (wt.%)	FeO(wt.%)
Around 10.5	7.21 ± 0.2	36.42 ± 0.7	12.78 ± 0.1	43.61 ± 0.2
Around 12	7.03 ± 0.3	37.07 ± 0.4	12.93 ± 0.6	42.97 ± 0.1
Around 13.5	7.57 ± 0.1	36.59 ± 0.7	12.58 ± 0.5	43.27 ± 0.3
Around 15	7.11 ± 0.1	35.36 ± 0.7	13.40 ± 1.2	44.13 ± 0.4
Average composition around 10-15 mm	7.23	36.36	12.92	43.49

4.1.4. Freeze lining from slag S2 with melilite as primary phase, 3 hours submergence time

There are 3 different layers in the freeze lining FL4 as seen in **Figure 4.8**. The overall thickness of FL4 is around 14 mm. The crystalline layer is present until around 12.5 mm from the probe. Then, until around 13 mm, there is a presence of an open crystalline layer. Afterwards, an entrained slag bath layer is present containing a low number of anorthite and spinel crystals.
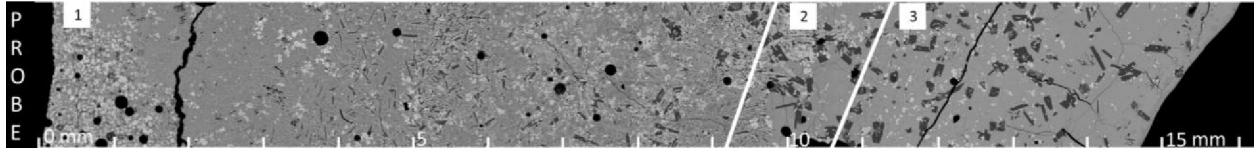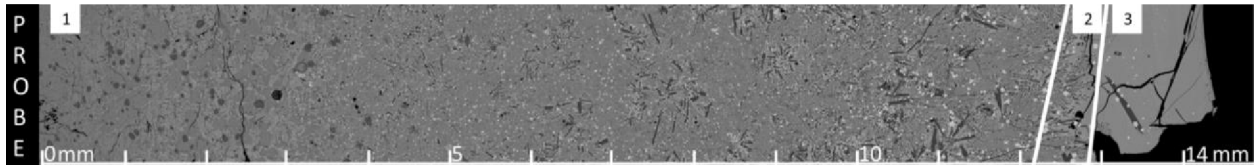
Figure 4.8: SEM-BSE stitched image of FL4 after 3 hours of submergence time. (1) Crystalline layer (2) Open crystalline layer (3) Entrained slag bath layer
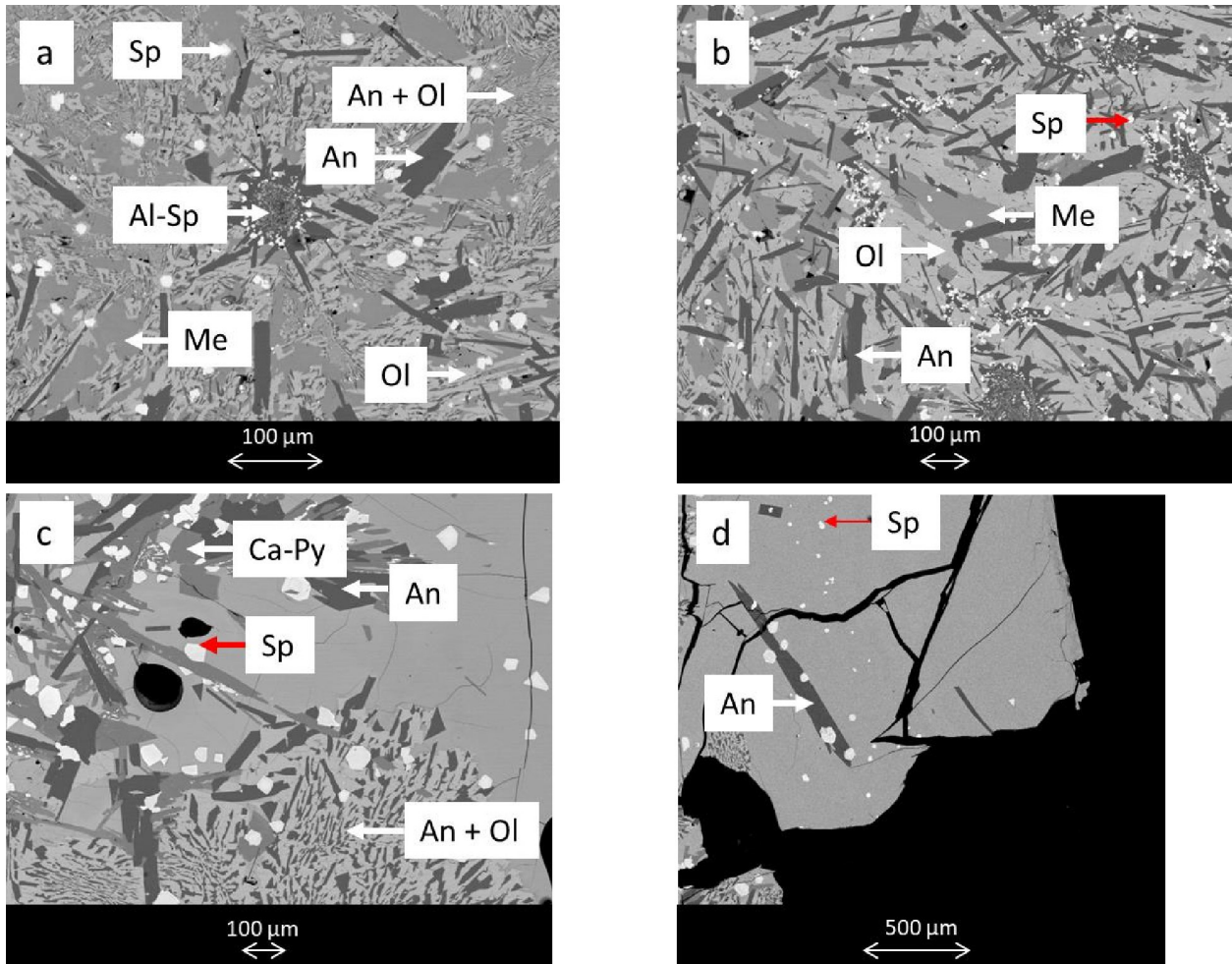
Figure 4.9: BSE images of FL4 showing the presence of different phases at certain distances from the probe. (a) Around 4 mm distance (b) Around 9 mm distance (c) Around 12 mm distance (d) Around 13.5 mm. An; anorthite, Ol; olivine, Sp; spinel, Me; melilite, An + Ol; anorthite + olivine, Al-Sp; Al_2O_3-enriched spinel, Ca-Py; Ca enriched pyroxene

The phases formed can be seen in **Figure 4.9**. Melilite was the first phase to be precipitated according to the FactSage thermodynamic equilibrium calculations. But when EBSD analysis was performed in a small zone of this freeze lining around 2 mm from the probe, the phase which is labelled as melilite in this freeze lining appeared to be the clinopyroxene phase but the results of EBSD analysis were complex and it was not 100% clear. When FactSage equilibrium calculations were performed while considering the global

46

composition of the freeze lining around 2 mm from the probe. It also predicted melilite phase to be the first phase which will precipitate under normal partial pressure of oxygen 10^{-12} ppm. Whereas these calculations predicted the precipitation of large amount of clinopyroxene phase after the small precipitation of spinel phase at higher partial pressure of oxygen 10^{-7} ppm. Hence, it could be possible that the actual partial pressure of oxygen during the formation experiment of this freeze lining was higher than normal. XRD analysis would have been a useful technique to clarify the identity of this phase but could not be performed at the time of this study. Based on the thermodynamic equilibrium predictions of FactSage, this phase is considered as melilite in this research.

In FL4 as seen in **Figure 4.9a**, the spinel phase is included in the anorthite phase, the anorthite phase is included in the melilite phase and the melilite phase is included in the olivine phase around 4 mm distance from the probe. This means spinel is precipitated first followed by respectively the precipitation of anorthite, melilite and then olivine and at the end Ca enriched pyroxene phase is precipitated around 12 mm distance from the probe in the region where the crystalline layer ends. Ca enriched pyroxene is known as clinopyroxene.

4.1.5. Comparison of freeze linings formed in a single primary phase field (FL1, FL2, FL3 & FL4)

The crystalline layer is thicker in the freeze linings formed in the melilite primary phase slag either after 3 hours or 30 minutes of submergence time compared to the freeze linings formed in the spinel primary phase slag. In FL3, the entrained slag bath layer is thicker than the entrained slag bath layer of FL4 which might be because of the high viscosity of slag system used to form FL3. Because of the high viscosity, the flowability of molten slag system used to form FL3 remains low, and it remained stuck to the freeze lining while pulling out the probe from the furnace at the end of the experiment followed by its quenching. The thickness of the crystalline layers is smaller in FL1 and FL2 in comparison to FL3 and FL4. As we prefer a thicker freeze lining to perform the transition experiments, 3 hours of submergence time was selected for FL5 and FL6 in which the transition from one primary phase field slag into another primary phase field slag was done.

The crystallization order of different phases in FL1 is different from FL3. The crystallization order of different phases is similar in FL2 and FL4. If we compare all the freeze linings from FL1 to FL4, the crystallization order of different phases is different from what was predicted through the FactSage simulations which is discussed above separately for these freeze linings in detail. This might have occurred

because of an undercool melt resulting from N2 cooled probe immersion in the molten bath. The formation of the first nuclei occurred from another phase than predicted by thermodynamic equilibrium calculations.
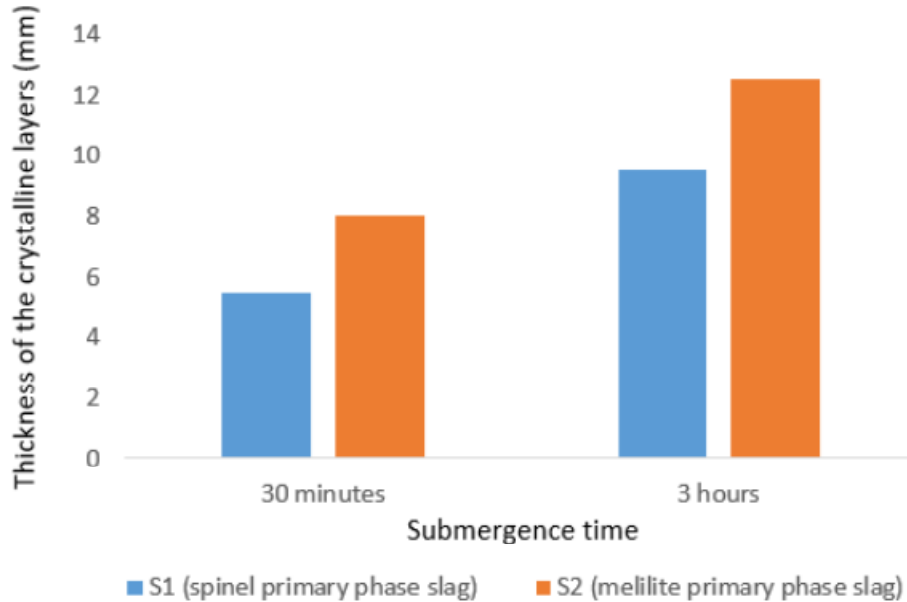
Figure 4.10: *Thickness of crystalline layers of the freeze linings based on submergence times in S1 & S2 slags.*

4.2 Microstructural study of the freeze linings obtained from the transition between two primary phase slags

In this paragraph, the freeze linings obtained from the transition experiments i.e., spinel primary phase to melilite primary phase and vice versa are analyzed to see the affect of the transition on the microstructure and the thickness of the freeze linings.

4.2.1 Freeze lining FL5: 3 hours immersion time in a spinel primary phase slag followed 3 immersion time in a melilite primary phase slag
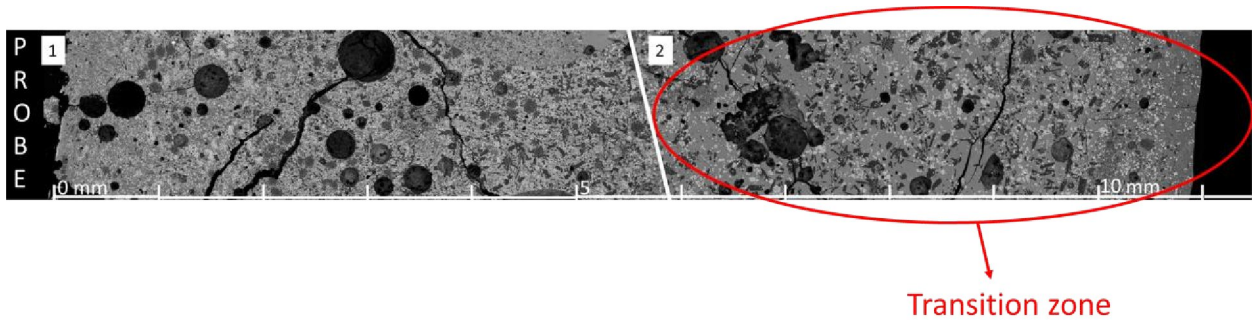
Figure 4.11: SEM-BSE stitched image of FL5. (1) Crystalline layer (2) Open crystalline layer

The thickness of the freeze lining FL5 is approximately 11 mm (**Figure 4.11**). There are 2 different layers in the freeze lining. The crystalline layer is present until around 6 mm from the probe. Then, an open crystalline layer **(Table 2.3)** is present until the end of the freeze lining where widely spaced spinel and anorthite phase crystals and a significant amount of solidified amorphous slag is present in between the open spaces around the crystals. There is a large amount of porosity present in the structure. Consequently, to avoid these large pores, the analysis were performed in a region with less pores, that is thinner than FL5's average thickness (the cross section is displayed in (**Figure 3.7d**). FL5 freeze lining is formed in 2 steps; formation of a freeze lining in spinel primary phase slag followed by its immersion in a melilite primary phase slag both for the duration of 3 hours. It shows the formation of the initial freeze lining in spinel primary phase slag is done with similar experimental parameters that were used to formed FL3. Hence, it becomes interesting to compare FL5 with FL3 to see what changes the transition from spinel primary phase slag to melilite primary phase slags has brought in the microstructure and the chemical composition of the freeze lining FL5. The thickness of FL5's crystalline layer appears to be around 6 mm for the analyzed thinner region instead of 9.5 mm in FL3.

4.2.1.a) Evidence of interaction between the intermediate freeze lining from FL5 with the new slag S2: overall freeze lining composition

Figure 4.12 shows the evolution in the composition of the freeze lining FL5 starting from the probe till the molten slag bath in comparison to the S1 and S2 slag compositions. The composition of FL5 is close to the S1 slag composition over the whole thickness of the freeze lining. Although the Al_2O_3 content is generally

49

higher in FL5 because the melting was done in an alumina crucible and the crucible's dissolution changed the initial slag composition. **Figure 4.13** presents the comparison of measured global compositions of respectively the freeze linings FL5 and FL3 over the whole thickness profile. The overall global composition of FL5 generally remains close to the global composition of FL3 over the whole thickness profile. It can be said, there is no formation of a freeze lining with S2 slag composition after the formation of intermediate initially formed freeze lining in S1 slag composition.

There are fluctuations in the composition curves based on the regions where the analysis was done to avoid porosities. The composition values could have been different if the analysis had been done in a slightly different region. The analysis was not done at equal distances to avoid the porosities.
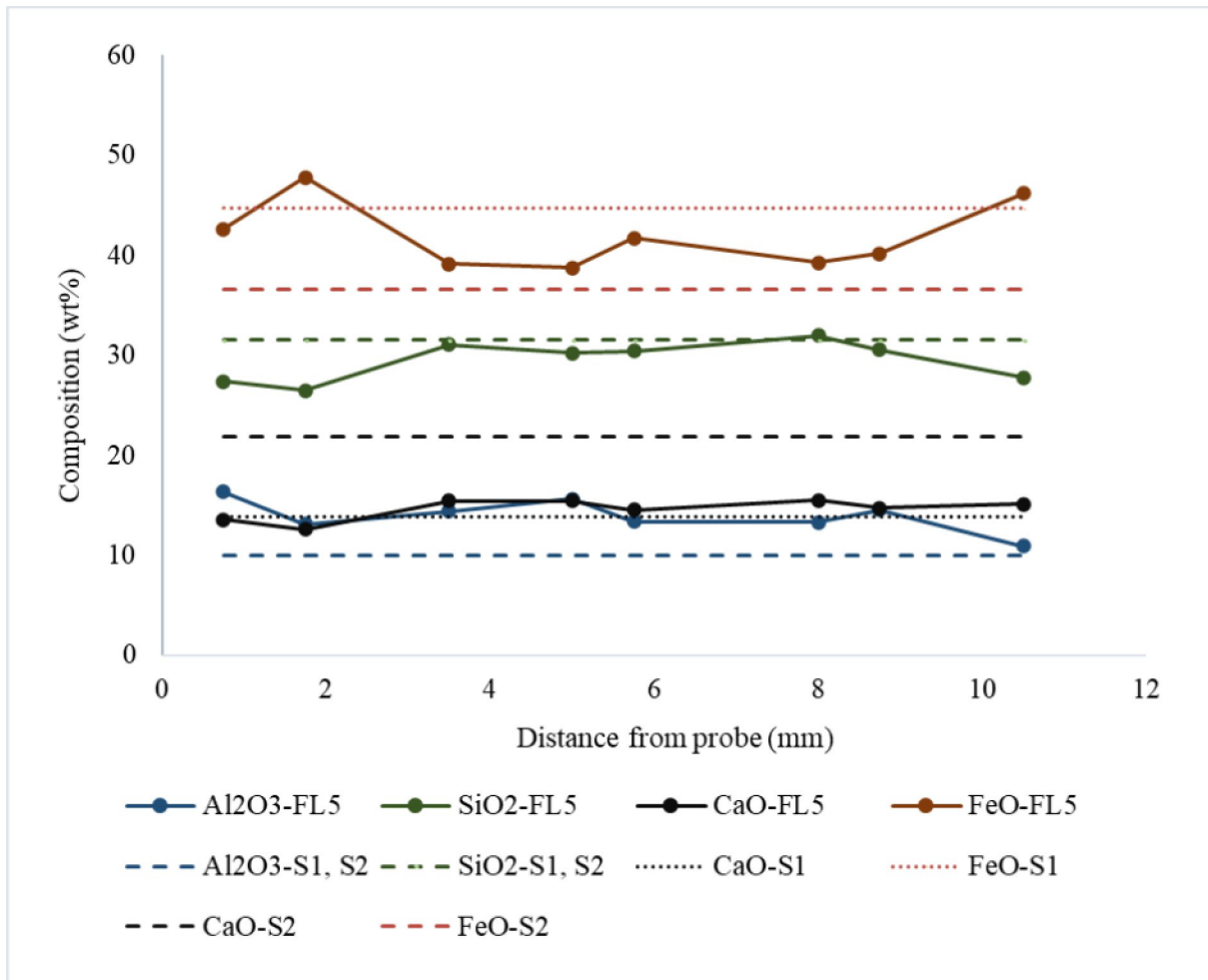
Figure 4.12: *EDAX analysis for the global composition of FL5 compared to the S1 & S2 whole slag composition.*
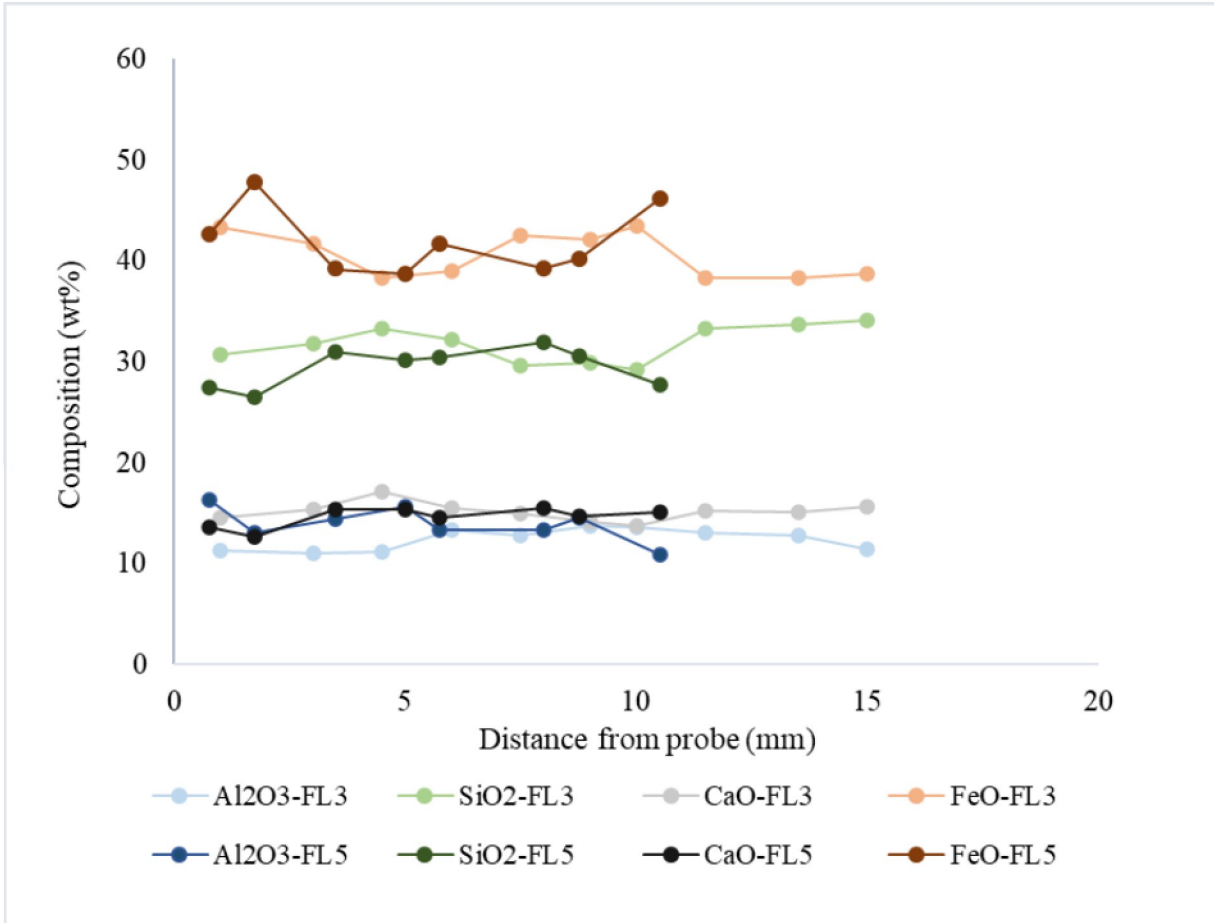
Figure 4.13: Comparison of the global composition of FL5 and FL3 over the whole thickness profile via EDAX analysis.

4.2.1.b) Evidence of the interaction between the intermediate freeze lining from FL5 with the new slag S2: chemical composition of the matrix at the interface of FL5

Table 4.4 shows the chemical composition of the solidified slag matrix in FL5 at different points between 6-11 mm distance from the probe and the average composition of the solidified slag matrix around 6-11 mm. The composition is measured via EDAX analysis. Based on this, it can be said that during the formation of FL5, the first freeze lining formed for 3 hours in S1 slag composition was quenched in water at room temperature. Hence the interface of this freeze lining was cold, and it started to heat up after submergence into the S2 molten slag. This caused the solidified slag matrix of the slag in the open crystalline layer and entrained slag bath layer of the initially formed freeze lining to melt and mix with the S2 slag. The local change in the slag composition led to a shift in the thermodynamic equilibrium and caused the formation of FL5 in a new thermodynamic equilibrium path around 6-11 mm distance from the probe. Before 6 mm distance from the probe, the FL5 grew on the thermodynamic equilibrium path which

is based on the S1 slag composition. Moreover, around 10-11 mm distance from the probe, the composition of the solidified slag matrix is slightly different from its composition around 6-10 mm distance from the probe. It means there is a precipitation of a new mineral in this region which is discussed later in this chapter.

Table 4-4: Measured composition of solidified slag matrix in FL5 at different points around 6-11 mm distance from the probe and the overall average composition.

Distance from Probe (mm)	Al_2O_3 (wt.%)	SiO_2 (wt.%)	CaO (wt.%)	FeO (wt.%)
Around 6	6.91 ± 0.2	36.31 ± 0.7	17.79 ± 0.1	39.00 ± 0.2
Around 7.5	7.14 ± 0.3	36.49 ± 0.4	17.82 ± 0.6	38.59 ± 0.1
Around 9	7.16 ± 0.1	36.23 ± 0.7	17.48 ± 0.5	39.13 ± 0.6
Around 10.5	6.83 ± 0.1	35.64 ± 0.7	16.90 ± 1.2	40.63 ± 0.4
Average composition around 6-11 mm	7.01	36.17	17.50	39.33

4.2.1.c) Evidence of interaction between the intermediate freeze lining from FL5 with the new slag S2: crystalline phases present at the interface of FL5

Figure 4.7c and **Figure 4.14c** shows the regions of respectively the freeze linings FL3 and FL5 at the interface between the crystalline layer and an open crystalline layer. The olivine phase present in these regions doesn't precipitate further causing an end to the growth of a crystalline layer in both freeze linings. Moreover, the phases formed in both freeze linings at earlier distances are identical (**Figure 4.7b**, **Figure 4.14b**). Hence, there is no change in the microstructure of FL5 after transition from S1 to the S2 slag bath in the crystalline layers of freeze linings.
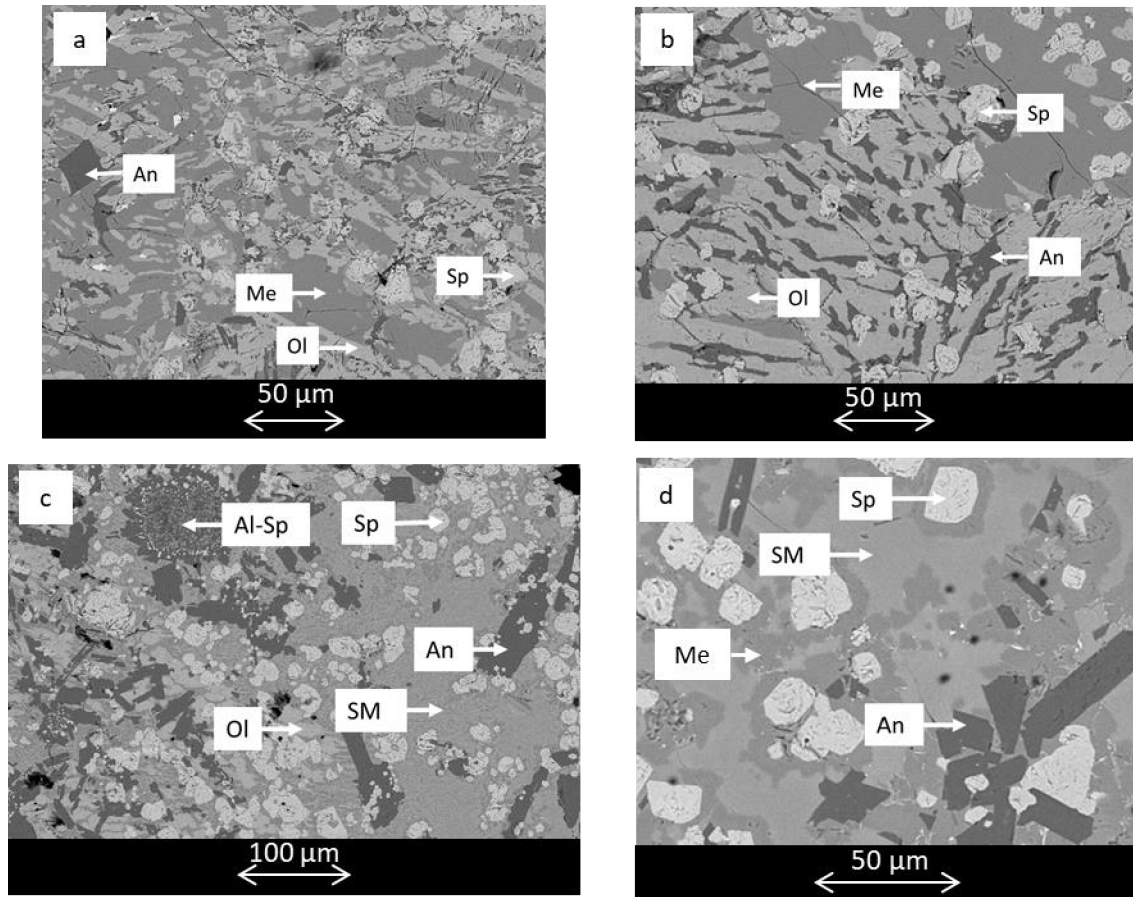
Figure 4.14: *BSE images of FL5 showing the presence of different phases at certain distances from the probe. (a) Around 0.5 mm distance (b) Around 3.5 mm distance (c) Around 6 mm distance (d) Around 10.5 mm distance. An; anorthite, Ol; olivine, Sp; spinel, Me; melilite*

Figure 4.15a shows the presence of large volume of porosities stuck in between the large number of crystals and the solidified slag matrix. An open crystalline layer is formed at the interface of FL5 around 6-11 mm as shown in **Figure 4.11**. In FL3 (**Figure 4.15b**) an entrained slag bath layer and an open crystalline layer was present with a lesser amount of isolated spinel and anorthite crystals with the solidified slag matrix of only S1 slag. Hence, the transition from S1 to S2 slag resulted in a denser crystalline layer at the interface of the freeze lining.
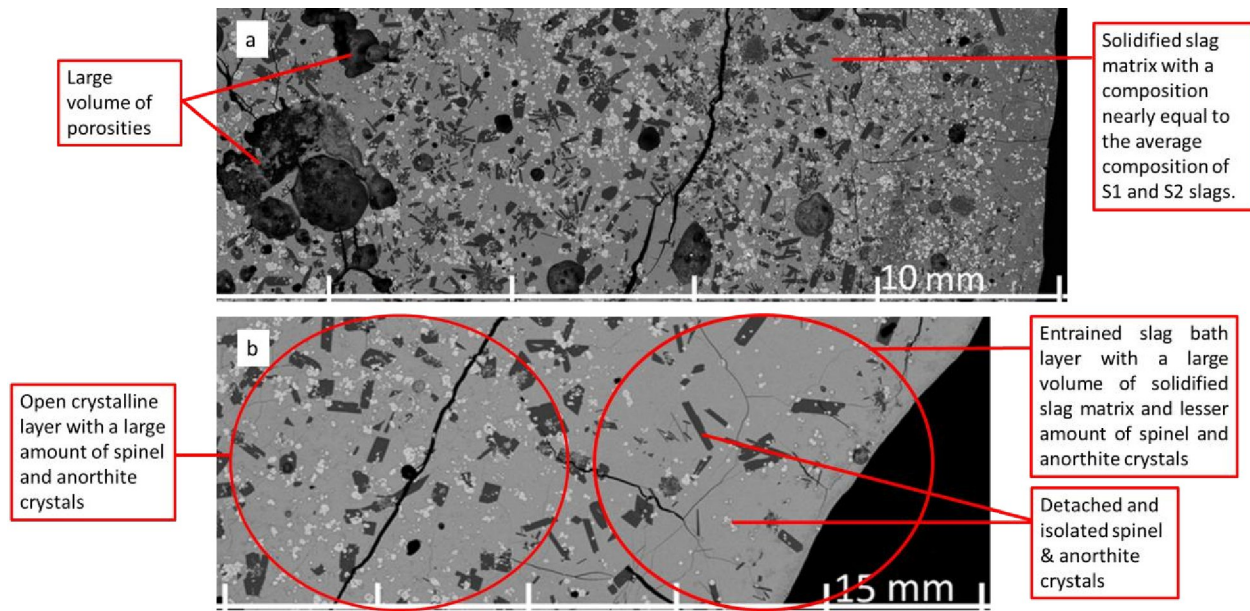
Figure 4.15: Magnified SEM-BSE images. (a) FL5 (b) FL3.

Spinel and Anorthite phases are present with the solidified slag matrix around 6-11 mm in FL5 **(Figure 4.15a)**. The composition of these 2 phases around 10.5 mm is almost similar to composition of these phases when formed in the crystalline layer of FL5 around 0.5, 3.5, and 6 mm distance from the probe (**Table 4.5**). Also, the composition of these 2 phases is similar to the composition of these phases when formed in the open crystallin layer of FL3.

Table 4-5: Average composition of the phases formed in the freeze lining FL5 at certain distances from the probe.

Distance from Probe (mm)	Phases formed	Al_2O_3 (wt.%)	SiO_2 (wt.%)	CaO (wt.%)	FeO(wt.%)
Around 0.5	Melilite	9.67 ± 0.5	41.02 ± 1.2	23.38 ± 0.1	25.93 ± 0.5
	Anorthite	35.90 ± 1.5	43.79 ± 1.9	20.31 ± 1.5	-
	Olivine	-	30.67 ± 0.5	14.82 ± 4.1	54.51 ± 3.9
	Spinel	13.53 ± 1.1	0.30 ± 0.0	-	86.17 ± 1.4
Around 3.5	Spinel	14.01 ± 0.7	-	-	85.99 ± 0.3
	Anorthite	36.32 ± 0.1	40.93 ± 0.4	20.24 ± 0.2	2.54 ± 0.3
	Olivine	-	31.21 ± 0.1	16.84 ± 1.5	51.96 ± 1.7

	Melilite	8.93 ± 0.4	40.51 ± 0.4	23.95 ± 0.3	26.61 ± 0.8
Around 6	Spinel	12.31 ± 1.5	-	-	87.69 ± 1.5
	Anorthite	36.19 ± 0.3	40.82 ± 0.4	20.30 ± 0.4	2.70 ± 0.2
	Olivine	-	30.70 ± 0.8	8.58 ± 0.5	60.72 ± 0.1
Around 10.5	Spinel	14.01 ± 0.1	-	-	86.00 ± 0.1
	Anorthite	36.43 ± 0.6	40.02 ± 0.5	20.68 ± 0.4	2.88 ± 1.0
	Melilite	9.70 ± 0.3	40.25 ± 0.1	23.38 ± 0.9	26.67 ± 1.5

This gives an indication that these phases are not newly formed after the transition but rather are the same phases which were already present in the freeze lining formed in slag S1 which was submerged in the S2 slag bath. The reason is the high level of stability of spinel [61] and anorthite crystals. Once they are formed it is difficult to dissolve them back into the slag. Hence, these 2 phases remained stable in FL5 around 6-11 mm after the transition of S1 to the S2. The melilite phase was not present around 6-10 mm in FL5 and it started to precipitate around 10.5 mm distance from the probe which can be seen in **Figure 4.14d**. This melilite phase is formed because of the transition from the S1 to S2 slag because the S2 slag composition is based on melilite as a primary phase. This phase was not present in the freeze lining FL3 in the region nearby the slag bath. The region where this melilite phase is precipitated is less than 1 mm in thickness and the freeze lining could not grow further in thickness after this region. That could be because of the S1 and S2 slag mixing and shift in thermodynamic equilibrium as discussed earlier.

Based on the microstructure, global composition, and the individual phase quantitative analysis, it can be concluded the initially formed intermediate freeze lining FL5 doesn't seem to have been deeply affected by the transition in a new slag composition S2, but only at its interface with the change in solidified slag matrix composition and the secondary precipitation of melilite around the spinel crystals. As it was expected based on study from Crivitis [53], there is no formation of a freeze lining with the overall global composition close to the S2 slag composition on top of the intermediate freeze lining formed in the S1 slag bath **(Figure 4.12, Figure 4.13)**. As the S1 and S2 slags were mixed at the interface of the intermediate freeze lining that changed the thermodynamic equilibrium path in which the freeze lining grew. This path is different from the one that was predicted for respectively the solidifications of S1 and S2 slags via FactSage equilibrium calculations.

4.2.2. Freeze lining FL6: 3 hours immersion time in a melilite primary phase slag followed by 3 hours immersion time in a spinel primary phase slag
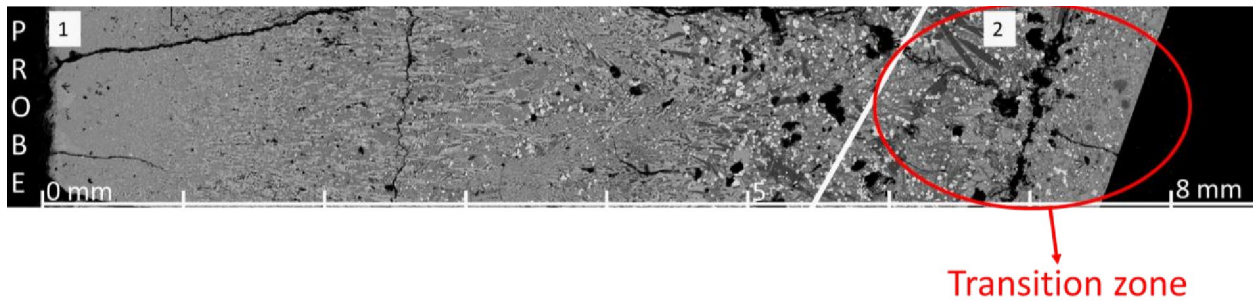
Figure 4.16: SEM-BSE stitched image of FL6. (1) Crystalline layer (2) Closed crystalline layer

The thickness of the freeze lining is approximately 7.5 mm (**Figure 4.16**). There are 2 different layers in the freeze lining. The crystalline layer is present until 5.5-6 mm from the probe. Then, a closed crystalline layer **(Table 2.3)** is formed until the end of freeze lining which mainly consists of crystals with a very small amount of the residual slag liquid solidified in between the spaces of the crystals. During the formation of FL6, the initially formed intermediate freeze lining with S2 slag composition was smaller in thickness compared to the thickness of the melilite primary phase freeze lining FL4. The reason for this is unknown. Therefore, the crystalline layer in FL6 appears to be only around 5.5-6 mm in thickness as compared to the approximately 12.5 mm thick crystalline layer in FL4.

The phases formed in FL6 around 1, 3, 6 and 7.5 mm from the probe and their respective average composition can be seen in **Figure 4.17** and **Table 4.6**. The microstructure of the crystalline layer formed in FL6 is identical to the microstructure of crystalline layer in FL4 showing the presence of same phases i.e., melilite, spinel, anorthite and olivine (**Figure 4.17b, Figure 4.9b**).
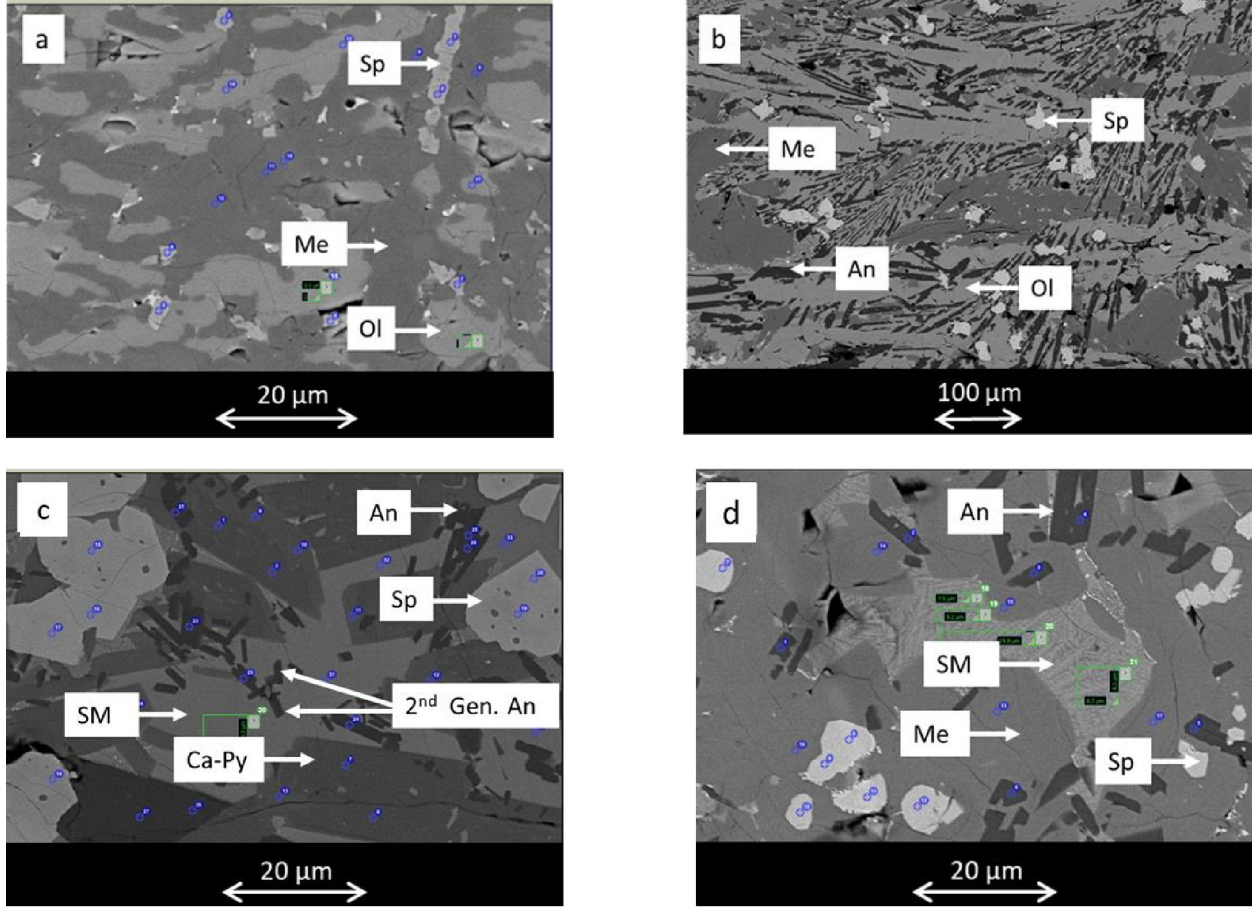
Figure 4.17: *BSE images of FL6 showing the presence of different phases at certain distances from the probe. (a) Around 1 mm distance (b) Around 3 mm distance (c) Around 6 mm distance (d) Around 7.5 mm. An; anorthite, Ol; olivine, Sp; spinel, Me; melilite, Ca-Py; Calcium enriched pyroxene, SM; solidified slag matrix*

Table 4-6: *Average composition of distinctive phases formed at specific distances starting from probe in the freeze lining.*

Distance from Probe	Phases formed	Al$_2$O$_3$ (wt.%)	SiO$_2$ (wt.%)	CaO (wt.%)	FeO(wt.%)
Around 1mm	**Spinel**	15.20 ± 5.7	0.56 ± 0.3	0.34 ± 0.2	83.90 ± 5.2
	Melilite	15.26 ± 1.0	38.70 ± 0.9	24.23 ± 0.4	21.81 ± 2
	Olivine	-	32.45 ± 0.2	27.53 ± 0.5	40.03 ± 0.6
Around 3mm	**Spinel**	14.67 ± 3.9	0.34 ± 0.1	0.43 ± 0.4	84.56 ± 4.9
	Anorthite	34.95 ± 0.4	41.28 ± 0.1	20.21 ± 0.5	3.57 ± 1.3

	Melilite	7.75 ± 0.0	43.14 ± 0.0	23.63 ± 0.0	25.48 ± 0.0
	Olivine	1.04 ± 0.1	31.82 ± 0.2	28.16 ± 0.1	38.99 ± 0.5
Around 6mm	Calcium Pyroxene	0.67 ± 0.6	51.33 ± 2.0	45.24 ± 5.6	7.87 ± 3.6
	Spinel	14.25 ± 2.0	1.00 ± 0.1	0.70 ± 0.0	84.65 ± 1.3
	Anorthite	34.62 ± 0.9	42.25 ± 0.3	21.06 ± 0.2	2.07 ± 0.4
	Solidified Slag Matrix	6.34 ± 0.3	34.94 ± 1.1	21.18 ± 1.0	37.55 ± 1.9
7.5mm	Anorthite	33.76 ± 0.3	42.02 ± 0.2	21.43 ± 0.2	2.79 ± 0.3
	Spinel	9.54 ± 0.5	1.96 ± 0.7	1.00 ± 0.3	87.65 ± 1.1
	Melilite	8.19 ± 0.5	41.85 ± 0.8	22.48 ± 0.1	27.49 ± 1.2
	Solidified Slag Matrix	5.48 ± 0.3	35.58 ± 0.1	17.77 ± 0.5	41.17 ± 0.5

Figure 4.18 shows the evolution in the composition of the freeze lining FL6 starting from the probe till the slag bath in comparison to the S2 slag composition. There are fluctuations in the composition curves based on the regions where the analysis was done to avoid porosities. The composition values could have been different if the analysis had been done in a slightly different region. The composition of FL6 is close to the S2 slag composition except the FeO content. Until around 2 mm from the probe, the FeO content remained lower and the SiO_2 content is higher compared to the S2 slag composition. it is because of the higher overall volume of melilite crystals in this region and small amount of spinel crystals as seen in **Figure 4.17a**. CaO content is also in higher amount compared to the S2 slag composition because of the melilite and olivine crystals. Between 2-5 mm, the content of CaO and SiO_2 remains almost constant. But there is an increase in the Al_2O_3 content while the FeO content decreases because of the anorthite precipitation and growth, the high volume of already present melilite crystals and the smaller volume of spinel crystals as seen in **Figure 4.17b**.
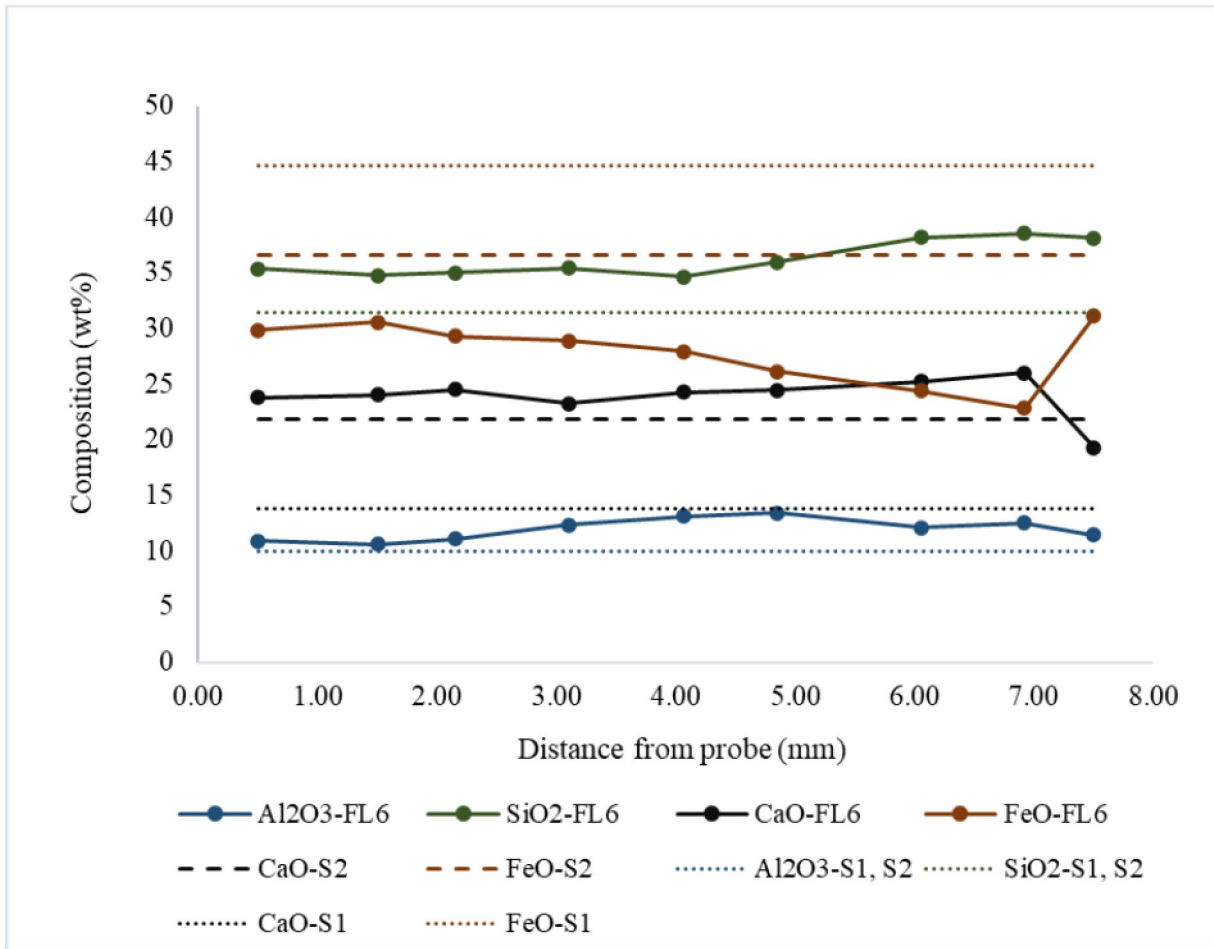
Figure 4.18: EDAX analysis for the global composition of FL6 compared to the S1 & S2 slag composition.

Between 5-7 mm, the FeO content continues to decrease and the Al_2O_3 content also decreases whereas the SiO_2 and CaO content increases, because the olivine crystals stopped growing after the end of the crystalline layer that is around 5 mm **(Figure 4.19)**. Also, Ca-enriched pyroxene crystals precipitated at the interface of the freeze lining with already present spinel and the anorthite crystals (**Figure 4.17c**). These phases are identical to the phases present at the interface of FL4. But in case of FL6, there is also a precipitation of second generation of isolated anorthite crystals (**Figure 4.17c**) which were not present at the interface of the crystalline layer in FL4 **(Figure 20b)**.
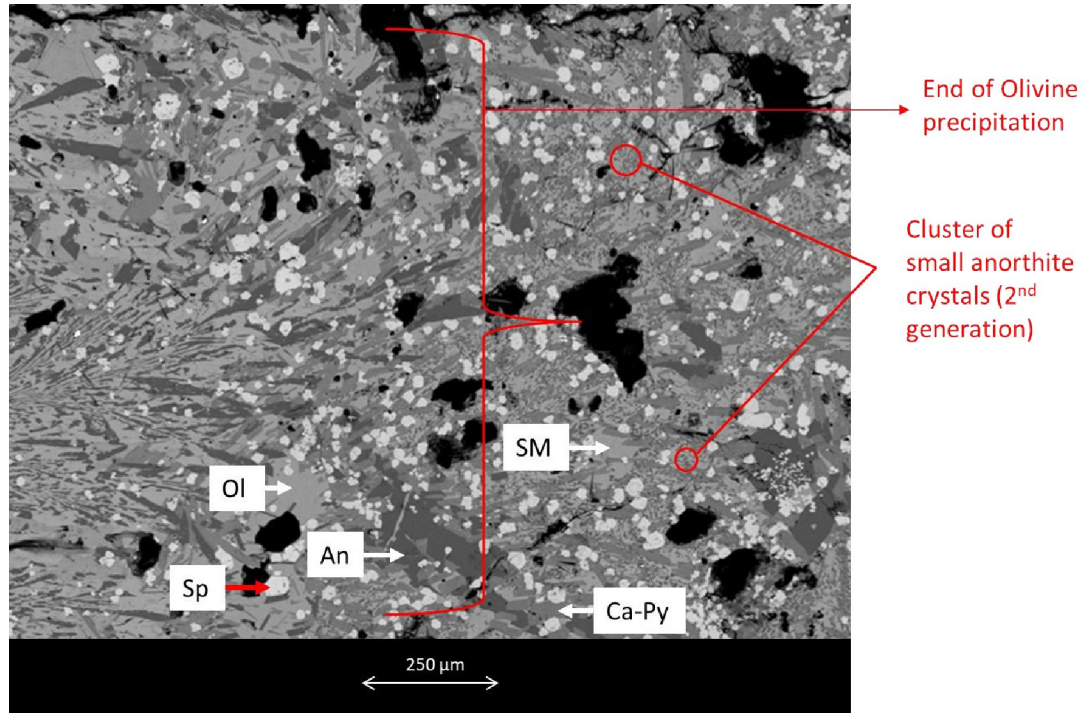
Figure 4.19: BSE image of FL5 showing the microstructure around 5 mm distance from the probe. Ol; olivine, Sp; spinel, An; anorthite, Ca-Py; Ca-enriched Pyroxene, SM; solidified slag matrix

In **Figure 4.18**, there is an abrupt increase in FeO content around 7.5 mm and a sharp decline in CaO content, because when the initially formed freeze lining in S2 slag composition was submerged into the slag bath of S1, it was at relatively low temperature, and it started to heat up after submergence. This caused the S2 slag present in the solidified slag matrix at the interface to melt and mix up with the S1 slag which changed the thermodynamic equilibrium path in which the freeze lining in S2 slag bath was growing because of the transition in the slag composition This thermodynamic equilibrium path is different from the one predicted via FactSage equilibrium calculation for the solidification of S2 slag bath. Whereas in FL4, the average of the measured composition of solidified slag matrix at the end of crystalline layer around 13.5 mm is almost similar to S2 whole slag composition **(Table 4.7)**.

Table 4-7: Average of the composition of solidified slag matrix around 13.5 mm (entrained slag bath layer) in FL4.

Al_2O_3 (wt.%)	SiO_2 (wt.%)	CaO (wt.%)	FeO(wt.%)
6.79 ± 0.2	35.09 ± 1.1	20.69 ± 1.0	37.43 ± 1.9

At the end of freeze lining towards the slag bath around 7-7.5 mm distance from the probe, FL6 grew with a mixed (S1 & S2) slag bath composition as discussed earlier due to the transition from S2 to S1 slag which led to the shift in the thermodynamic equilibrium. Hence, there is a precipitation of large volume of melilite crystals with already present undissolved, spinel and stable anorthite crystals (both generations) and a small amount of the solidified slag matrix to form a closed crystalline layer **(Figure 4.20a)**. Ca-enriched pyroxene crystals stopped growing before the region where melilite crystals started precipitation **(Figure 4.20a)**. In FL4 before transition, An open crystalline layer is present at the interface where Ca-enriched pyroxene crystals stopped growing and after that point, an entrained slag bath layer is present towards slag bath with the presence of spinel and anorthite crystals with a large volume of the solidified slag matrix at the interface **(Figure 4.20b)**. Melilite phase and the second generation of anorthite crystals are formed after the transition in FL6 **(Figure 4.20a)**. The closed crystalline layer formed in FL6 after the transition from S2 to S1 slag is much denser compared to a less dense freeze lining at the interface before the transition. Moreover, as it was expected based on the study from Crivitis [53], there is no growth of freeze lining with overall global composition close to the S1 slag composition on top of initially formed intermediate freeze lining with S2 slag composition after the transition **(Figure 4.18).**
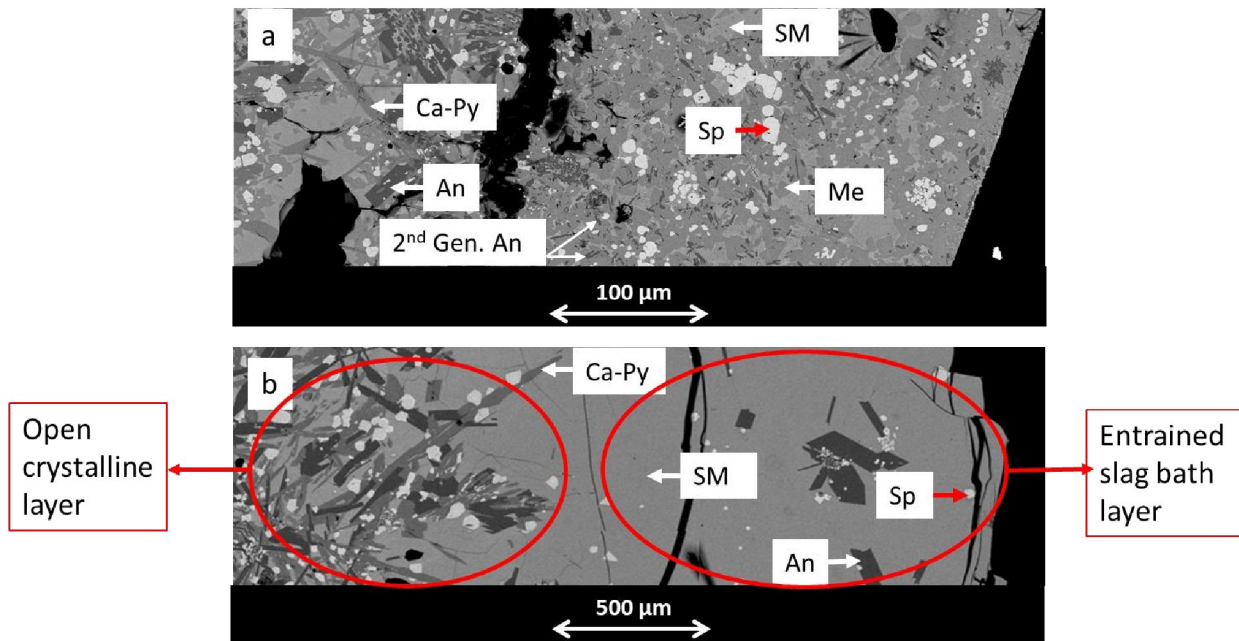

Figure 4.20: *Magnified SEM-BSE images. (a) FL6 around 7-7.5 mm (b) FL4 around 12.5-14.5 mm Sp; spinel, An; anorthite, Me; melilite, Ca-Py; Ca-enriched pyroxene, SM; solidified slag matrix*

5. Conclusion

The main objective was to analyze the behavior of a freeze lining immersed in a slag with a different primary phase than the one it was originally formed. This is critical to understand in case in case of recycling smelting refineries that are protected by the freeze linings, such refineries are treating batch feeds of secondary raw materials coming from various sources, and with various compositions. Hence, there is a strong chance that the slag bath may alter, and it is important to understand how this would affect the already-formed freeze linings. A synthetic SiO_2-FeO-CaO-Al_2O_3 slag system is used in this study to form the freeze linings. Two slag compositions are selected through thermodynamic calculations with the software FactSage: spinel primary phase slag (S1) and the melilite primary phase slag (S2). Firstly, freeze linings are formed for 30 minutes of formation times in both the slag compositions respectively (FL1 & FL2). Then, 3 hours of formation time was applied to form the freeze linings in both the slag compositions respectively (FL3 & FL4). The 3 hours of formation time was chosen for the transition experiments. There were 2 freeze lining's formation experiments realized for the transition between primary phase slags, the spinel primary phase slag to melilite primary phase slag freeze lining (FL5), and vice versa (FL6).

Varying submergence times of N_2-cooled stainless-steel probe in a slag bath affects the freeze lining formation. In this research, it is found out when freeze linings are formed for 3 hours of the submergence time, the crystalline layers of the freeze linings are thicker compared to their thickness after submergence for 30 minutes. Moreover, freeze linings formed in melilite primary phase slag grow much thicker as the crystalline layer is thicker compared to the freeze linings formed in spinel primary phase slag.

FL5 remained the same in terms of the microstructure and composition until the end of crystalline layer as compared to FL3. The solidified slag matrix of the entrained slag bath layer of the intermediate freeze lining (similar to FL3) from FL5 melted at high temperature when submerged in S2 slag bath. These 2 molten slags (S1&S2) got mixed up and due to the compromised slag composition, there was a shift in thermodynamic equilibrium path from the original path which was predicted for the S1 slag composition. That led to the change in solidified slag matrix composition in the open crystalline layer around 6-11 mm in FL5. There was no growth of freeze lining with melilite primary phase slag composition on top of initially formed intermediate freeze lining with spinel primary phase slag composition. But there was precipitation of the new melilite crystals in the region nearby the slag bath. In context of industrial application, if there is a transition of slag composition from spinel primary phase to melilite primary phase, a denser open crystalline layer is formed with a precipitation of new melilite crystals.

The microstructure of the crystalline layer formed in FL6 is identical to the microstructure of the crystalline layer in FL4, with the same mineral phases present. Due to the immersion of the initially formed intermediate freeze lining (similar to FL4) from FL6 in the S1 slag bath, the phases increased in size and a closed crystalline layer is formed with a lesser amount of solidified slag matrix at the interface around 7 mm distance from the probe. There is a formation of second generation of the anorthite crystals at the interface of FL6 which was not the case in FL4. The solidified slag matrix of the entrained slag bath layer initially formed intermediate freeze lining (similar to FL4) melted at high temperature when submerged in S1 slag bath. Then, S1 & S2 mixed up and changed the thermodynamic equilibrium path. This path is different from the path which was predicted for the S2 slag composition. Consequently, new melilite crystals are precipitated in the region nearby the slag bath in FL6. There was no growth of a freeze lining with S2 slag composition on top of initially formed freeze lining with S1 slag composition. In context of the industrial application, if there is a transition of slag composition from melilite primary phase to spinel primary phase, there is a denser closed crystalline layer formed at the interface of the freeze lining with the presence of newly precipitated large volume of melilite crystals with the precipitation of 2nd generation of anorthite crystals.

The crystalline layers of the initially formed intermediate freeze linings in both the transition experiments remained similar in composition and microstructure compared to what was achieved respectively in FL3 and FL4. Moreover, these initially formed intermediate freeze linings remained stable after the transition which suggests a good protection of the furnace walls and the lance material slag wear.

Possible future work to continue the research in this domain could be:

- Slag composition of recycling smelting refineries are as well based on different other primary phases than melilite and spinel. Multiple studies can be done focusing on the transitions among these other primary phase slags. That includes melilite to olivine; olivine to melilite; spinel to olivine; olivine to spinel etc. These studies will provide a much clearer understanding of freeze linings behaviors under changing slag batch compositions.
- The rotation of crucible can be applied in future, it will provide near industrial conditions during the experiments.
- The end slag samples remaining in the crucible after the formation of the freeze linings could be collected and analyzed. This will give information on evolution of the overall slag composition during the freeze lining formation, and on the mineral phases precipitated in the molten bath and freely floating in it.

6. References

[1] EuRICMetalRecyclingFactsheet.

[2] Dessart, F.J. and L. Bontoux, Non-ferrous metals manufacturing: vision for 2050 and actions needed, Publications Office of the European Union, Luxembourg, 2017.

[3] https://www.umicore.com/storage/migrate/2010CMD_Hoboken.pdf.

[4] P.L. Duncanson and J.D. Toth, THE TRUTHS AND MYTHS OF FREEZE LINING TECHNOLOGY FOR SUBMERGED ARC FURNACES, https://www.pyrometallurgy.co.za/InfaconX/062.pdf.

[5] Crivits, T., Hayes, P.C. and Jak, E., An investigation of factors influencing freeze lining behaviour, Mineral Processing and Extractive Metallurgy 127 (2018), 4, pp. 195–209.

[6] Campforts, M., Verscheure, K., Boydens, E., van Rompaey, T., Blanpain, B. and Wollants, P., On the Microstructure of a Freeze Lining of an Industrial Nonferrous Slag, Metall and Materi Trans B 38 (2007), 6, pp. 841–851.

[7] Hofer, O. / Klima, R. / Altland, R. / Beckmann, B. / Grabietz, H.-G, On-line wear determination for improved life-time of blast furnace hearth based on heat-ux meters, 3rd International Conference.

[8] Jan Torrkulla, H.S., Model of the State of the Blast Furnace Hearth 40 (2000), pp. 438–447.

[9] J.H. Zietsman, Interactions between Freeze Lining and Slag Bath in Ilmenite Smelting, PhD thesis, 2004.

[10] P.C. Pistorius, Fundamentals of freeze lining behaviour in ilmenite smelting (2003), pp. 509–514.

[11] Kenneth C. MILLS, Yuchu SU, Alistair B. FOX, Zushu Li, A Review of Slag Splashing 45 (2005), pp. 619–633.

[12] Camp, J. M. James McIntyre and 1858-1927, The Making, Shaping and Treating of Steel.

[13] AHMED H A, EL-RAGHY S M ELREFAIE F A, REDA S BASSUNY Z, Prediction of the thermal aspects of egyptalum prototype high-amperage pre-baked aluminum reduction cells. (1994), pp. 333–338.

[14] T. E. Fletcher,T. A. Utigard &P. Desclaux, Determination of the Heat Transfer Coefficient between Molten Cryolite and a Solid Surface 35 (2013), pp. 53–59.

[15] Lindsay, S.J., Light Metals 2011, John Wiley & Sons, Inc, Hoboken, NJ, USA, 2011.

[16] Solheim, A., Some Aspects of Heat Transfer Between Bath and Sideledge in Aluminium Reduction Cells, in: S.J. Lindsay (Ed.), Light Metals 2011, John Wiley & Sons, Inc, Hoboken, NJ, USA, 2011, pp. 381–386.

[17] Verscheure, K., High-Temperature Zinc Fuming in Water-Cooled Reactors - Thermodynamic Modeling and Experimental Investigation (Hoge Temperatuur Zink Verdamping in Watergekoelde Reactoren - Thermodynamische Modellering En Experimentele Studie), leuven, 2007.

[18] https://www.totalmateria.com/page.aspx?ID=CheckArticle&site=ktn&NM=358

[19] https://www.isasmelt.com/en/download/Brochures/ISASMELT%20Brochure.pdf.

[20] M Floyd and D S Conochie, SIROSMELT: The first ten years, in Extractive Metallurgy Symposium, Melbourne Branch, 1984.

[21] T Shibasaki, K Kanamori and M Hayashi, Development of (sic) large scale Mitsubishi furnace at Naoshima, Savard/Lee International Symposium on Bath Smelting .

[22] P Bartsch, C R Fountain and B Anselmi, Radio Hill Project, Perth, Western Australia, 1990.

[23] Shirish Thakre. Kumaresan Thangaraj, D Shah, Design modification using CFD to improve the performance of the waste heat boiler (2011).

[24] Technology, G., ISASMELT™ – 2020 Compendium of Technical Papers.

[25] Solnordal, C.B., Jorgensen, F.R.A. and Taylor, R.N., Modeling the heat flow to an operating sirosmelt lance, Metall and Materi Trans B 29 (1998), 2, pp. 485–492.

[26] Verscheure, K., Furnace Cooling Technology in Pyrometallurgical Processes (Keynote).

[27] R_v_Laar, Microsoft Word - Blast Furnace Lining and Cooling Technology - Plate Cooler Designs, AISE 2003.doc.

[28] K.E. Scholey, I.V. Samasekera and G.G. Richards, Thermal Stress Failure of Water Cooled Zinc Fuming Furnace Jackets, Can. Metall. Quart 33 (1994), pp. 77–84.

[29] G. Slaven, A. MacRae and L. Valentas, The Implementation of UltralifeTM Copper Casting Technology in the EAF, Paper presented at AISE, Pittsburg.

[30] Plascencia, G., Utigard, T.A. and Jaramillo, D., Extending the life of water-cooled copper cooling fingers for furnace refractories, JOM 57 (2005), 10, pp. 44–48.

[31] Bellemans, Inge, Johan Zietsman, and Kim Verbeken. "Fundamental and Formation Aspects of Slag Freeze Linings: A Review." *Journal of Sustainable Metallurgy* (2022): 1-27.

[32] Fallah-Mehrjardi, Ata, Peter C. Hayes, and Evgueni Jak. "Investigation of freeze-linings in copper-containing slag systems: Part I. Preliminary experiments." *Metallurgical and Materials Transactions B* 44, no. 3 (2013): 534-548.

[33] Verscheure, Karel, Mieke Campforts, Frederik Verhaeghe, Eddy Boydens, Bart Blanpain, Patrick Wollants, and Maurits Van Camp. "Water-cooled probe technique for the study of freeze lining formation." *Metallurgical and Materials Transactions B* 37, no. 6 (2006): 929-940.

[34] Jansson, J., Pekka Taskinen, and Markku Kaskiala. "Freeze lining formation in continuous converting calcium ferrite slags. I." *Canadian Metallurgical Quarterly* 53, no. 1 (2014): 1-10.

[35] Kalliala, Olli, Markku Kaskiala, Tuija Suortti, and Pekka Taskinen. "Freeze lining formation on water cooled refractory wall." *Mineral Processing and Extractive Metallurgy* 124, no. 4 (2015): 224-232.

[36] D.G.C. Robertson, S.K., Model studies of heat transfer and flow in slag-cleaning furnaces (1999), pp. 157–158.

[37] Campforts, Mieke, Karel Verscheure, Eddy Boydens, Tim Van Rompaey, Bart Blanpain, and Patrick Wollants. "On the mass transport and the crystal growth in a freeze lining of an industrial nonferrous slag." *Metallurgical and Materials Transactions B* 39, no. 3 (2008): 408-417.

[38] Campforts, M., Jak, E., Blanpain, B., & Wollants, P. (2009). Freeze-lining formation of a synthetic lead slag: Part I. Microstructure formation. *Metallurgical and Materials Transactions B*, *40*(5), 619-631

[39] C. Orrling, Y. Kashiwaya, S. Sridhar, and A.W. Cramb, In sity observations and thermal analysis of crystallization phenomena in mold slags (2000).

[40] Campforts, M., Blanpain, B., & Wollants, P. (2009). The importance of slag engineering in freeze-lining applications. *Metallurgical and Materials Transactions B, 40(5), 643-655*

[41] Mills, Kenneth C., Yuchu Su, Alistair B. Fox, Zushu Li, Richard P. Thackray, and H. T. Tsai. "A review of slag splashing." *ISIJ international* 45, no. 5 (2005): 619-633.

[42] Fallah-Mehrjardi, Ata, Peter C. Hayes, and Evgueni Jak. "Understanding slag freeze linings." *JOM* 66, no. 9 (2014): 1654-1663.

[43] Fallah-Mehrjardi A, Hayes PC, Jak E (2013) Investigation of freeze linings in copper-containing slag systems: Part II. Mechanism of the deposit stabilization. Metall Mater Trans B 44(3):549–560

[44] Crivits T, Hayes PC, Jak E (2018) Investigation of the efect of bath temperature on the bath-freeze lining interface temperature in the CuOx-FeOy-MgO-SiO2 system at copper metal saturation. Int J Mater Res 109(5):386–398

[45] Verscheure, K., Campforts, M., Verhaeghe, F., Boydens, E ., Blanpain, B., Wollants, P. and van Camp, M., Water-cooled probe technique for the study of freeze lining formation, Metall and Materi Trans B 37 (2006), 6, pp. 929–940.

[46] Fallah-Mehrjardi, A., Jansson, J., Taskinen, P., Hayes, P.C. and Jak, E., Investigation of the Freeze-Lining Formed in an Industrial Copper Converting Calcium Ferrite Slag, Metall and Materi Trans B 45 (2014), 3, pp. 864–874.

[47] ITEE, Investigation of Freeze Linings in Copper Containing Slag Systems.

[48] Energy of Explosions Occurring when Water Falls onto a Layer of Molten Metal.
[49] Fallah-Mehrjadi, A., Hayes, P. C., & Jak, E.(2013). Investigation of freeze lining in copper-conta18ining slag systems: high-temperature experimental investigation of the effect og bath agitation." Metallurgical and Materials Transactions B, 44(6), 1337-1351, 619-631.

[50] Investigation of Bath/Freeze Lining Interface Temperature Based on the Rheology of the Slag

[51] Fallah-Mehrjardi, Ata, Peter C. Hayes, and Evgueni Jak. "Investigation of freeze linings in copper-containing slag systems: Part II. Mechanism of the deposit stabilization." *Metallurgical and Materials Transactions B* 44, no. 3 (2013): 549-560.

[52] Slag Valorisation Symposium, Proceedings of the 6th International Slag Valorisation Symposium.

[53] Crivitis, T., Zhang L., Chen L., Malfliet A., 2019, Evolution of freeze linings

in multi-step processes, San Antonio, Texas, USA, 10-14 March (yet to be published)

[54] Crivits T, Hayes PC, Jak E (2018) Freeze linings in the Al2O3– CaO–SiO2 system. Int J Mater Res 109(7):638–653

[55] Fallah-Mehrjardi A, Hayes P, Jak E (2014) Further experimental investigation of freeze-lining/bath interface at steady-state conditions. Metall Mater Trans B 45(6):2040–2049

[56] K. Verscheure, M. Van Camp, B. Blanpain, P. Wollants, P. Hayes, and E. Jak: Metall. Mater. Trans. B, 2007, vol. 38B, pp. 13–20.

[57] P.C. Pistorius: JSAIMM, 2004, vol. 104 (7), pp. 417–22.

[58] Fallah-Mehrjardi, A., Hayes, P. and Jak, E., Further Experimental Investigation of Freeze-Lining/Bath Interface at Steady-State Conditions, Metall and Materi Trans B 45 (2014), 6, pp. 2040–2049.

[59] Samant, Mathias Chintinne, Muxing Guo, and Bart Blanpain. "Investigation of Bath/Freeze Lining Interface Temperature Based on the Rheology of the Slag." *Jom* 74, no. 1 (2022): 274-282.

[60] https://www.webmineral.com/

[61] McClane, Devon L., et al. "Dissolution of Accumulated Spinel Crystals in Simulated Nuclear Waste Glass Melts." *Journal of Hazardous, Toxic, and Radioactive Waste*, vol. 22, no. 2, Apr. 2018.